https://doi.org/10.5194/egusphere-2026-6733
Preprint. Discussion started: 13 November 2026
© Author(s) 2026. CC BY 4.0 License.

Balloon-based trace gas observations reveal Asian Summer Monsoon impact in the UTLS over Germany

Johannes C. Laube[1], Christian Rolf[1], Attahir Mainika[1], Andreas Engel[2], Markus Geldenhuys[3,4], Bärbel Vogel[1], Thomas Wagenhäuser[2], and Michaela I. Hegglin[1,5,6]

[1]Institute of Climate and Energy Systems: Stratosphere (ICE-4), Forschungszentrum Jülich, Jülich, 52425, Germany
[2]Institute for Atmospheric and Environmental Sciences, Goethe University of Frankfurt, Frankfurt, Germany
[3]South African Weather Service, 1263 Heuwel Road, Centurion, South Africa
[4]Institute for Coastal and Marine Research, Nelson Mandela University, Gqeberha, 6001, South Africa
[5]Institute for Atmospheric and Environmental Research, University of Wuppertal, Wuppertal, Germany
[6]Department of Meteorology, University of Reading, Reading, UK

Correspondence to: Johannes C. Laube (j.laube@fz-juelich.de)

Abstract. For many important trace gases, precise observations in the upper troposphere and lower stratosphere (UTLS) are spatially and/or temporally sparse and/or inhomogeneous. This is particularly limiting in the UTLS as a highly variable transition region between the troposphere and stratosphere. We here present a new and unique dataset obtained from weather balloon-based sensors across the summer of 2025. Between 27th May and 5th November, 46 balloons were launched on an almost weekly basis from near Jülich, Germany, typically reaching altitudes of around 30 km. Of those flights, 37 focused on trace gases, with 18 near-simultaneous double launches quantifying the vertical distribution of water vapour and ozone as well as multiple halogenated species; thus, enabling access to the temporal evolution of many key UTLS components over a period of about five months. We here focus mainly on ozone-depleting chlorinated very short-lived substances (Cl-VSLSs) with model-based surface-origin tracers to investigate the source regions of the air masses. In particular, we investigate the influence of the Asian Summer Monsoon region - a source of Cl-VSLSs such as CH_2Cl_2 - as the upper-level anticyclone exports air masses into the global northern hemispheric UTLS during the monsoon season. We find that the "background" lower stratospheric composition in summer and autumn is clearly impacted by the Asian monsoon-related stratospheric entrance pathway, and for Cl-VSLSs much more so than estimated in previous studies.

1 Introduction

As the atmospheric abundances of most longer-lived ozone-depleting substances (ODSs) are decreasing (Laube and Tegtmeier, 2023; Western et al., 2025), the contribution of chlorinated very short-lived substances (Cl-VSLSs) to stratospheric ozone depletion has gained increasing attention in recent years (e.g., Claxton et al., 2019; Hossaini et al., 2019). Cl-VSLSs have comparably short atmospheric lifetimes of less than six months, and are, in contrast to other ODSs, not regulated by the Montreal Protocol on Substances that Deplete the Ozone Layer (Laube and Tegtmeier, 2023). Notably, a

https://doi.org/10.5194/egusphere-2026-6733
Preprint. Discussion started: 13 November 2026
© Author(s) 2026. CC BY 4.0 License.

recent satellite-model-based study highlighted their importance as it was estimated that Cl-VSLSs have reduced the observed decrease in inorganic stratospheric chlorine by 25%–30% during 2004–2020 (Dubé et al., 2025).

Emissions of Cl-VSLSs such as dichloromethane (CH_2Cl_2) and chloroform ($CHCl_3$) have been rising in some regions, especially in the eastern and southern parts of Asia (e.g., Claxton et al., 2019; Fang et al., 2019; Say et al., 2019; Zhang et al., 2026). This is of particular importance as the Asian Summer Monsoon can transport air masses into the stratosphere much more rapidly compared to the main entry pathway via the tropical tropopause (e.g. Vogel et al., 2016; Müller et al., 2016; Rolf et al., 2018; Riese et al., 2025; Yan et al., 2025); circumventing a more pronounced decay of Cl-VSLSs in the troposphere and therefore enabling a higher contribution to the chlorine loading of the stratosphere.

Accordingly, several aircraft-based studies have found substantially enhanced mole fractions of Cl-VSLSs in the upper troposphere and lower stratosphere in the vicinity of the Asian Summer Monsoon Anticyclone (ASMA; Adcock et al., 2021; Pan et al., 2024; Jesswein et al., 2025; Vogel et al., 2026) as well as in monsoon-influenced air over the Atlantic Ocean and Europe (Lauther et al., 2022). At the same time, modelling studies have aimed to shed more light on the global impact of such emissions. Claxton et al. (2019) found that Southeast Asian emissions have, due to their vicinity to the ASMA, up to a factor of 3 times greater potential to deplete stratospheric ozone than European ones; while Liang et al. (2025) estimated that the monsoon anticyclone "is the primary pathway for Very-Short-Lived Chlorocarbons (Cl-VSLSs) to enter the stratosphere" with simulated August peak abundances (when the ASMA is strongest) found to inject more than double (~200 ppt Cl) the amount injected in the tropics into the stratosphere in 2022.

However, due to the high variability of Cl-VSLS mole fractions in the upper troposphere and lower stratosphere (UTLS) on the one hand (CH_2Cl_2: 29-600 ppt, $CHCl_3$: 6-60 ppt; Laube and Tegtmeier, 2023; Pan et al., 2024; Vogel et al., 2026), and the lack of spatial and temporal coverage by observations on the other, the actual contribution of Cl-VSLSs to stratospheric chlorine from the ASMA entry route remains poorly constrained to date. The 2025 BAMBI campaign (Backyard Asian Monsoon Balloon Investigation) of the JUelich Modular Balloon Observatory (JUMBO) was designed to shed further light on this issue. JUMBO itself is a collection of miniature sensors and samplers that can be flown in different combinations – depending on the scientific question – on weather balloons (Geldenhuys et al., 2024). In this case, the main aim was to track the evolution of the "background" composition and potential ASMA influence of various trace gases in the UTLS over the several months, via balloon launches in Europe, i.e. far from the ASMA. Similar influences of the ASMA have already been found for multiple other trace species in the northern hemispheric stratosphere in summer (e.g., Vogel et al., 2016; Müller et al., 2016; Khaykin et al., 2017; Rolf et al., 2018; Wetzel et al., 2021, Graßl et al., 2024).

As demonstrated in Laube et al. (2025), up to 30 halogenated species can be quantified in AirCore-derived stratospheric air samples. The focus of this work is however on Cl-VSLS and the influence of Asian Monsoon-related air, which is why only a subset of the 10 most relevant species are being discussed here: Three Cl-VSLSs (CH_2Cl_2, $CHCl_3$, C_2Cl_4), and seven further gases that help placing the data in dynamical and chemical context (CFC-11, H-1211, HCFC-22, HFC-125, and SF_6, plus H_2O and O_3). The BAMBI campaign data complements previous aircraft-based observations, which have only covered short periods of time and were often limited in altitude ranges.

https://doi.org/10.5194/egusphere-2026-6733
Preprint. Discussion started: 13 November 2026
© Author(s) 2026. CC BY 4.0 License.

2 Methods

Results are based on two different sensor packages (see 2.1 and 2.2) launched near Jülich, Germany (50.90844° N, 6.41368° E, 85 m a.s.l.) using weather balloons. The first flight on 27th May 2025 only lifted one package (see 2.2), whereas the remaining 36 flights were all near-simultaneous (within 30 mins of each other) double launches. The core campaign period was from 12th June to 7th October 2025, i.e. covering most of the monsoon season as well as the decay of the ASMA. During this time flights took place on a weekly basis, the only exception being the w/c 18th July due to instrument repairs. Also, an "encore" post-monsoon double launch took place on 5th November 2025, i.e., about 4 weeks after the end of the main campaign. More campaign details including all flight dates, altitude ranges covered, and recovery times, can be found in the supplement (Table S1).

2.1 AirCores, subsampling, and air sample analysis

AirCores are cost-effective passive sampling devices that have become an established method to collect vertical profiles of air at altitudes between ~35 km and the ground (e.g., Karion et al., 2010; Membrive et al., 2017; Wagenhäuser et al., 2021; Tans, 2022). If recovery is swift (i.e., within a few hours after landing), air collected at different altitudes will not have experienced significant internal mixing despite being part of the same sample. This is largely due to the diffusion-limiting internal dimensions of AirCores, with typical tubing lengths around 100 m, and internal diameters of 1/8 - 1/4 inches. The AirCore flown as part of the BAMBI campaign consisted mainly of two pieces of coiled thin-walled tubing (tropospheric end: ~8.5 m of 1/2 inch tubing with inner diameter of 11.684 mm; stratospheric end: ~85 m of 1/8 inch tubing with inner diameter of 2.921 mm), with a total internal volume of 1.264 litre.

Once recovered, AirCores can be analysed for their trace gas content directly, e.g. by using fast optical spectroscopy methods (Karion et al., 2010). Should analysis not be feasible on site or be too time-intensive, it is possible to conserve the vertical information by decanting the air into subsampling devices (e.g., Mrozek et al., 2016; Laube et al., 2020). This was the case during BAMBI, with two subsamplers utilised to refill the stratospheric and upper tropospheric part of the AirCore (No. 1: 14 loops @ 20 ml, 1 @ 50 ml; No.2: 10 loops @ 20 ml, 3 @ 35 ml, 2 @ 50 ml). The total internal volumes of these two devices were intentionally different (330 ml vs 405 ml), so that the subsampled air reached from the top altitude down to across the tropopause regardless of its pressure altitude on a launch day. This endeavour was successful for almost all flights, with one exception: On 8th July, an unexpectedly high-pressure low-altitude tropopause (~355 hPa) was encountered, and therefore no AirCore-based data is available at and below the tropopause. Also, two measures were employed for quality assurance purposes: a) the subsampler internal stainless-steel surfaces were coated with Silco™-1000 for optimal trace gas inertness, and b) the average storage time between the filling of the subsampler and the measurements was relatively short (3 days, range: 1-12 days, Table S1). Both are known to improve trace gas data quality, especially for shorter-lived species, which can experience concentration changes when stored in sampling canisters or subsamplers for longer time periods (e.g., Laube et al., 2008, 2025).

https://doi.org/10.5194/egusphere-2026-6733
Preprint. Discussion started: 13 November 2026
© Author(s) 2026. CC BY 4.0 License.

Also, a gas not currently present in the atmosphere (i.e., perfluoro triethylamine, PFTEA) was added to the N_2 filled into the AirCore prior to the launch. This enabled the quantification of the exact fraction of air that remained in the AirCore at top altitude. The exact subsampling and fill gas content correction methodology, including subsequent altitude assignment of the collected air, has recently been described in detail in Laube et al. (2025). All subsampled air was analysed via Gas Chromatography-Mass Spectrometry (GC-MS) using a high-sensitivity system with the exact same methodology as in Laube et al. (2025). Table 1 contains a list of all trace species discussed here, including formulas, average precisions and calibration scales.

Table 1 Details of the species discussed in the manuscript including average precisions (over the entire campaign period) of repeats of the "working standard" (i.e., a clean air sample purchased from the NOAA Global Monitoring Labs in 2019) as well as AirCore-based samples (all from the upper troposphere). Differences in those precisions can mainly be attributed to differences in mole fractions, with especially C_2Cl_4 often exhibiting abundances close to detection limits in the samples (0.04 – 1.2 ppt). Data for all species (including ground-based mole fractions from Taunus Observatory, and model-based ones from Liang et al., 2025, which are both linked to AGAGE scales) were converted onto consistent calibration scales, following a recent lab calibration intercomparison exercise (Laube et al., 2025).

Trace Gas (formula)	Average Aircore precision (%)		Ground-based	Calibration scale linked
	Standards	Sample repeats	uncertainty*	to
CFC-11 ($CFCl_3$)	0.6	0.4	0.1	NOAA 2016 GC-ECD
H-1211 (CF_2ClBr)	1.6	1.5	0.8	NOAA 2006 GC-ECD
HCFC-22 (CHF_2Cl)	0.8	0.4	0.1	NOAA 2006 GC-MS
HFC-125 (C_2HF_5)	0.7	0.7	1.4	UB-98
SF_6	1.0	0.7	1.2	NOAA 2014 GC-ECD
Dichloromethane (CH_2Cl_2)	0.8	2.3	4.5	NOAA 2003 GC-MS
Chloroform ($CHCl_3$)	3.9	3.2	5.0	NOAA 1992 GC-MS
Perchloroethylene (C_2Cl_4)	2.3	9.1	18	NOAA-2003B

*includes measurement precisions and atmospheric variability not removed by the baseline filter (see 2.4)

2.2 Ozonesonde and Cryogenic Frost point Hygrometer

Unlike other trace gases, water vapor and ozone can be measured very effectively in situ during balloon flights. A total of three instruments were used here for this purpose. A Vaisala RS41-SGP radiosonde collected meteorological data such as temperature, pressure, and humidity, as well as GPS location from which winds can be calculated. This device also enables all measurement data to be transmitted via radio to the ground station. The temperature sensor of the RS41 radiosonde has an uncertainty of 0.3 K below 16 km and 0.4 K above. The uncertainty of the humidity sensor is given as 3 % (in relative humidity), and the pressure sensor has an uncertainty of 1.0 hPa at ambient pressure above 100 hPa, 0.3 hPa between 10 and 100 hPa, and 0.04 hPa below 10 hPa (Vaisala, 2020; Dirksen et al., 2020).

https://doi.org/10.5194/egusphere-2026-6733
Preprint. Discussion started: 13 November 2026
© Author(s) 2026. CC BY 4.0 License.

Ozone volume mixing ratios were measured using an electrochemical concentration cell (ECC) ozonesonde (Smit et al., 2007), which has an uncertainty of approximately 5 % below 20 km altitude (Smit et al., 2007; Thompson et al., 2019; Tarasick et al., 2021). Water vapor concentrations in the tropopause region and lower stratosphere were measured with a cryogenic frost point hygrometer (CFH; Vömel et al., 2007, 2016). To replace the previously used, phased-down refrigerant R23 (CHF_3), we developed a modified CFH that uses liquid nitrogen (LN_2) from a pressurized reservoir maintained at approximately 200 mbar above ambient pressure, preventing LN_2 freezing at low ambient pressures and maintaining efficient mirror cooling during ascent. This new cooling system was flown alongside the previous one on multiple occasions before the BAMBI campaign and exhibited comparable performance. The CFH is particularly well suited for measuring the very low water vapor concentrations encountered near the tropopause and throughout the stratosphere, providing reliable observations up to altitudes of approximately 28 km with an uncertainty of about 4 % in the troposphere and less than 10 % in the stratosphere (i.e. approx. 0.5 ppmv; e.g. Vömel et al. 2016; Khordakova et al., 2022).

For two of the BAMBI-2025 flights carrying the Water Vapor and Ozone Payload (25th June 25 and 11th September), instrument problems occurred at launch, resulting in no CFH-based water vapor data being available for those days. Instead, the water vapor mixing ratios were determined from radiosonde relative humidity measurements. A previous comparison of the RS41 radiosonde with the CFH found a dry bias at higher altitudes, i.e., 3 %–6 % (0.1–0.5 ppmv) at 80–120 hPa, and 9 % (0.4 ppmv) at 60–80 hPa (Jorge et al. 2021). The BAMBI data of the flights with measurements from both sensors yields somewhat higher discrepancies towards higher pressures, i.e., 17 % / 1.8 ppmv at 120-200hPa, 12 % / 0.6 ppmv at 80-120 hPa, and 9 % / 0.4 ppmv at 60-80 hPa. Given the aforementioned uncertainties associated with both instruments, the RS41 nevertheless provides reasonably reliable measurements of water vapor in the UTLS. We have consequentially used it as a substitute for the two dates where CFH data is unavailable.

2.3 Setup of the Chemical Lagrangian Model of the Stratosphere (CLaMS)

A global 3-dimensional simulation using the Chemical Lagrangian Model of the Stratosphere (CLaMS) (McKenna et al., 2002a, b; Pommrich et al., 2014, and references therein) was performed to study the origin of air masses of the BAMBI measurements. The simulation was started on 1st May 2025, during the pre-monsoon period, and covers the entire Asian summer monsoon season and autumn of 2025. The model was driven by winds from the ERA-5 reanalysis (Hersbach et al., 2020).

The CLaMS simulation includes 32 different regional model tracers of surface origin (hereafter referred to as 'surface–origin tracers') that together cover the entire Earth's surface as introduced in Vogel et al., 2026. These surface–origin tracers are released in the model boundary layer (approximately 2–3 km above the surface, accounting for orography) every 24 h and are subsequently advected and mixed into the free atmosphere over the course of the CLaMS simulation.

Vogel et al., 2026 introduced a marker for air from the Asian summer monsoon region and refer to it as the South Asia (SA) tracer (a sum of different surface-origin tracers, Fig. 1) that is largely confined within the ASMA. In contrast, air masses

https://doi.org/10.5194/egusphere-2026-6733
Preprint. Discussion started: 13 November 2026
© Author(s) 2026. CC BY 4.0 License.

from adjacent regions – particularly from Southeast Asia and the western Pacific – tend to be located near the edge of the ASMA (e.g. Vogel et al., 2019, 2026) and are summarised as the Western Pacific (WP) tracer (Fig. 1).

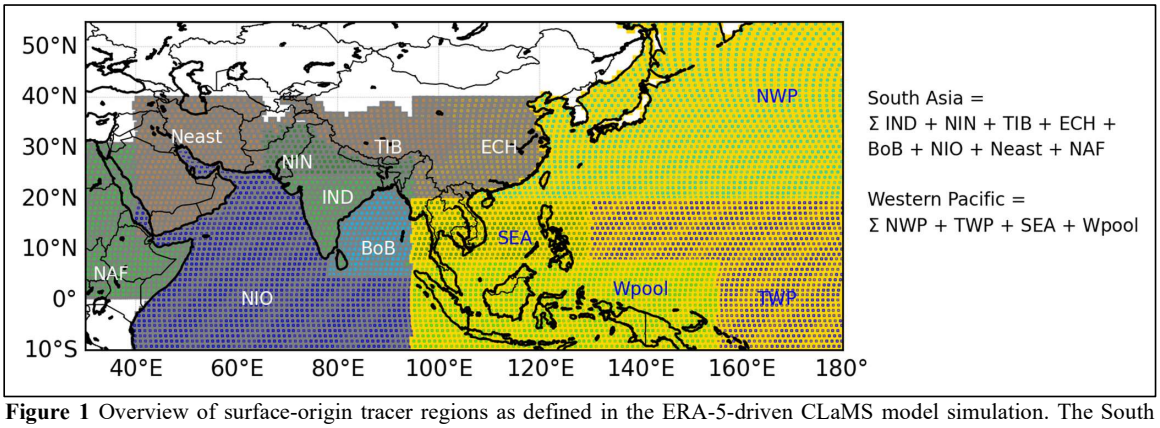


Figure 1 Overview of surface-origin tracer regions as defined in the ERA-5-driven CLaMS model simulation. The South Asia (SA) tracer is defined as the sum of several surface-origin tracers in the Asian summer monsoon region (TIB + IND + NIN + ECH + BoB + NIO + Neast + NAF) and serves as a good proxy for the ASMA (grey background). The Western Pacific (WP) tracer (SEA + Wpool + TWP + NWP) is a good indicator of air uplifted into the UTLS by tropical cyclones in the western Pacific (yellow background, adapted from Vogel et al., 2026).

2.4 Ground-based observations at Taunus Observatory

At the Taunus Observatory, atmospheric dry-air mole fractions of more than 50 halogenated trace gases have been measured in situ since February 2023 as part of the AGAGE program (Prinn et al 2018, https://www-air.larc.nasa.gov/missions/agage/). The observatory is relatively close to the launch site in Jülich as it is located in a rural area on top of the mountain Kleiner Feldberg at 50°13'19"N and 8°26'47"E, elevated 825 m above sea level. Two-litre air samples are collected through an inlet extending 12 m above ground level and measured in situ using a Medusa GC-MS system (Miller et al. 2008). Details on the specific setup are given in Meixner et al. (2025). Typical measurement precisions are given in Table 1.

Measurement data collected between 2024 and early 2026 have been processed using the IAU baseline filter (Schuck et al., 2018, available at https://zenodo.org/records/18668744) to derive a “background” mixing ratio function. Details on this baseline filter are given in Schuck et al. (2018). In principle, a function combining a polynomial and a seasonal term is fitted to the data. Points falling outside a defined scatter range are flagged as outliers and excluded from the next iteration, after which the function is refitted. This process repeats until the residual does not change by more than 10 % compared to the

https://doi.org/10.5194/egusphere-2026-6733
Preprint. Discussion started: 13 November 2026
© Author(s) 2026. CC BY 4.0 License.

previous iteration. The uncertainty of the background mixing ratio function is taken as the mean of the residuals from the final iteration's fit.

3 Results and discussion

3.1 Halogenated trace gases with a focus on chlorinated VSLS

Trace gases, especially longer-lived ones, have long been known to exhibit compact correlations in the stratosphere (e.g., Solomon et al., 1992; Volk et al., 1996). Figure 2 shows the results from the entire campaign as correlations between CFC-11 and H-1211, and CH_2Cl_2. The compactness of the data can be viewed as an indication of its quality, alongside the relatively small measurement uncertainties that are also shown. Especially noticeable is that in the vicinity of the tropopause (equivalent to all CFC-11 mixing ratios >200 ppt) H-1211 and CH_2Cl_2 show very different variability ranges: 2.4-2.8 ppt (~17 %), and 43-149 ppt (~250 %), respectively. This is reflective of H-1211 being a much longer-lived gas (total lifetime: 16 years, Burkholder and Hodnebrog, 2023) with virtually no tropospheric sinks (SPARC, 2013) while at the same time very few atmospheric sources remain to date (Laube and Tegtmeier, 2023, Western et al., 2025). On the other hand, the shorter lifetime of CH_2Cl_2 (176 days, range 95-1070 days, Burkholder and Hodnebrog, 2023) already causes a much less uniform atmospheric distribution, and this is exacerbated by its sources having surpassed 1000 Gg yr^{-1} globally (Laube and Tegtmeier, 2023; Zhang et al., 2026). Also notable in Fig. 2 is that the relative rate of decay higher up in the stratosphere (< 180 ppt of CFC-11) starts slowing down much earlier for CH_2Cl_2. While transport effects do of course play a role here, this is caused mainly by the differences in the locations of the dominant sink reactions, i.e. stratospheric photolysis for H-1211, as opposed to reaction with OH (of which there is much less in the stratosphere) for CH_2Cl_2. This example nicely illustrates the sometimes-confusing effects from differences in local and global trace gas lifetimes.

https://doi.org/10.5194/egusphere-2026-6733
Preprint. Discussion started: 13 November 2026
© Author(s) 2026. CC BY 4.0 License.

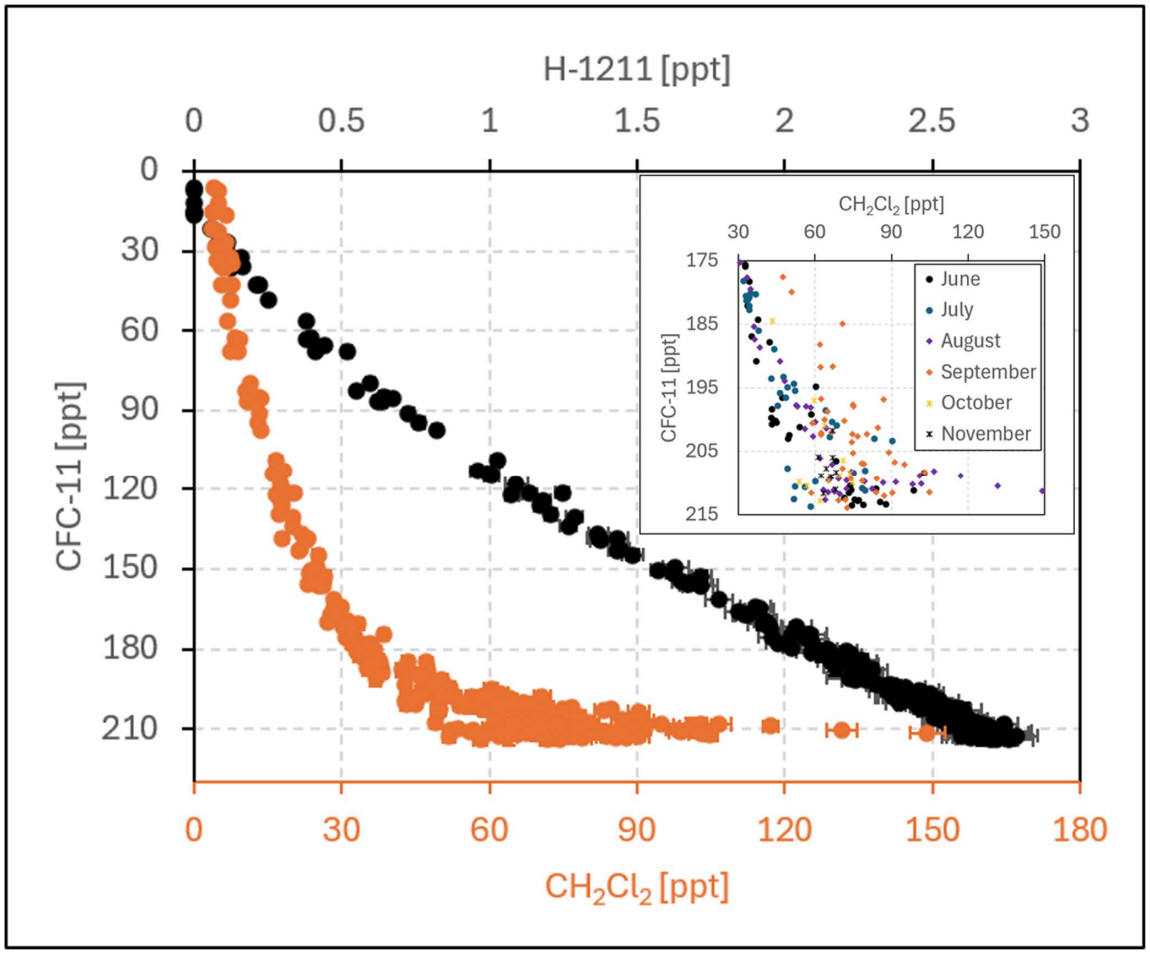


Figure 2 Correlation of CFC-11 mixing ratios in the upper troposphere and stratosphere with those of H-1211 (black), and CH_2Cl_2 (orange) for all AirCore flights of the 2025 BAMBI campaign. Generally, the lower the mixing ratio, the deeper the air was in the stratosphere. The tropopause is located approximately around 210 ppt of CFC-11. Error bars shown are derived from the measurements as one standard deviation (see 2.1) and are in many cases too small to be discernible. The inset shows a zoom-in on the UTLS region for the CFC-11-CH_2Cl_2 correlation with the colouring representing the flight month.

Already visible in the inset of Fig. 2 is the tendency of CH_2Cl_2 to exhibit higher mole fractions in the UTLS with progressing campaign duration. To investigate the temporal and spatial variability of the trace gases of interest in this region in more detail, an altitude range relative to the tropopause (derived as the first thermal tropopause using the WMO definition) is advisable as tropopause heights can vary considerably even on short timescales. Figure 3 shows curtain plots of CFC-11,

https://doi.org/10.5194/egusphere-2026-6733
Preprint. Discussion started: 13 November 2026
© Author(s) 2026. CC BY 4.0 License.

HCFC-22, HFC-125, and SF_6 across the campaign period. Potential temperature is used as a common vertical range indicator in this region (although similar figures with altitude on the y-axis are available in the supplement for convenience). Some variability is visible, especially occasional descent of air masses from higher up leading to lower mixing ratios (e.g., on 26th August). These are more pronounced for species with stronger chemical sinks in the stratosphere, in this case predominantly CFC-11. Within the "background" Lowermost Stratosphere (LMS, at 20-50 K) a temporal increase is perceptible, especially for gases with stronger current tropospheric sources such as HFC-125 and SF_6. This is not unexpected due the known phenomenon of the seasonal flushing of the extratropical lowermost stratosphere by relatively young, tropospherically influenced air, associated with enhanced summertime and autumnal quasi-isentropic transport from the tropical and subtropical upper troposphere across the subtropical jet region into the LMS (Hegglin and Shepherd, 2007; Bönisch et al., 2009). This transport pathway can be strongly influenced by air masses with origin from the Asian summer monsoon region, contributing to the flushing (Vogel et al., 2016; Rolf et al., 2018). Because of the lack of sinks for those two gases in the UTLS region, the corresponding mixing ratio enhancements are essentially cumulative over the timescale of the campaign, if somewhat tempered by the mixing effect with stratospheric "background" air. Also notable is that below the tropopause these enhancements over time are substantially less pronounced. Finally, in the layer immediately above the tropopause, extending to around 20-30K, the trace gas concentrations are indicative of the Extratropical Tropopause Transition Layer (ExTL, Hegglin et al., 2009; Gettelman et al., 2011) with strong influence from vertical and quasi-horizontal in-mixing from the underlying troposphere. This feature is more clearly evident in trace gases with stronger gradients across the tropopause such as in ozone and water vapour (Fig. 5).

https://doi.org/10.5194/egusphere-2026-6733
Preprint. Discussion started: 13 November 2026
© Author(s) 2026. CC BY 4.0 License.

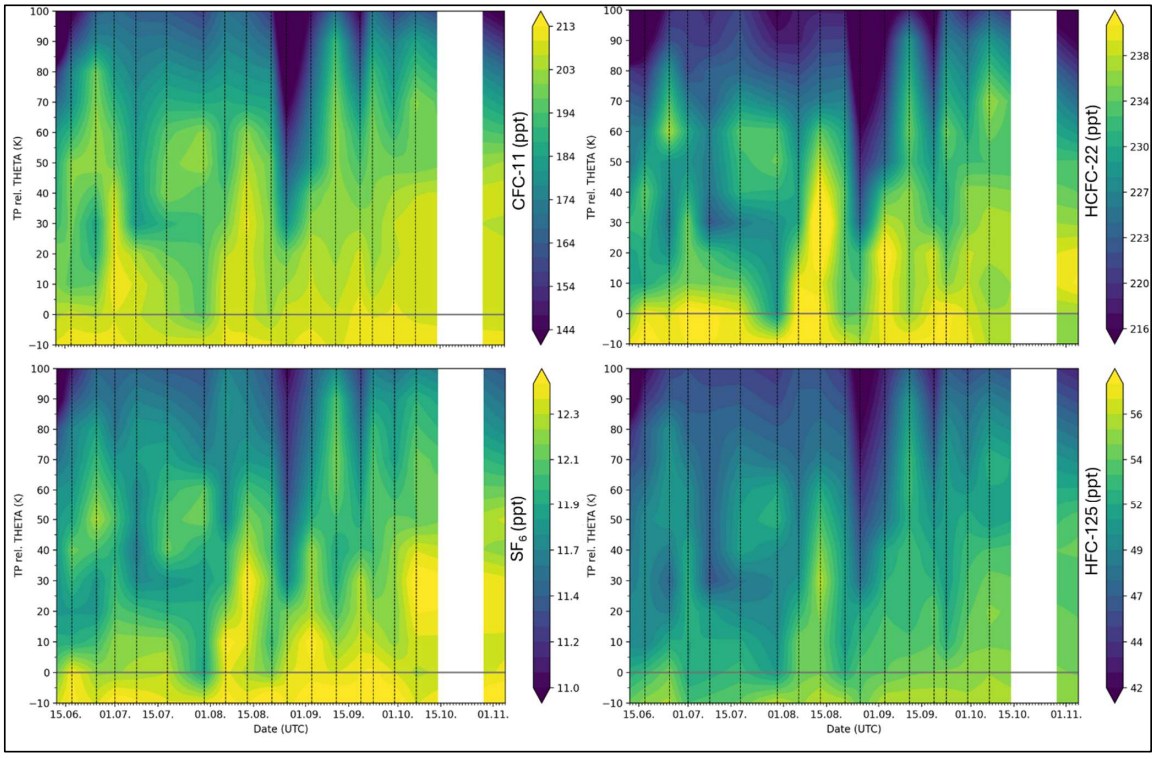


Figure 3 Curtain plots of observed mixing ratios during the BAMBI 2025 campaign for CFC-11 (upper left), HCFC-22 (upper right), HFC-125 (lower left), and SF_6 (lower right). Note that colour scales are representative of a different mixing ratio range for each gas. The vertical axis is potential temperature relative to the thermal tropopause (zero, solid line). Individual balloon flights are indicated by dashed vertical lines, with linear interpolation between them. The white area in October was intentionally left unfilled due to the longer period (~ 4 weeks) between the last two flights.

Similar curtain plots for CH_2Cl_2 and $CHCl_3$ (Fig. 4) yield a picture that is, initially, less straightforward to interpret. This is mainly due to a strong mixing ratio enhancement event around 30 K on 13th August dominating the colour scale. The corresponding anomaly plots (also Fig. 4) do however reveal a picture similar to that observed for the longer-lived species in Fig. 3, i.e. distinct stratospheric mixing ratio enhancements towards the second half of the campaign. As already seen in Fig. 2, the enhancements for CH_2Cl_2 – and here, $CHCl_3$ – are much more pronounced in a percentage sense. This is in line with current understanding of where such enhanced mixing ratios in the lower stratosphere are typically coming from. If they were indeed entirely related to the tropospheric "flushing" mechanism, the observed enhancements should not be that high as both CH_2Cl_2 and $CHCl_3$ have strong inner-hemispheric gradients. If the sole driver of such "flushing" was isentropic transport from the upper troposphere in the subtropics (e.g., Ploeger et al., 2013 and 2017), this should therefore lead to

https://doi.org/10.5194/egusphere-2026-6733
Preprint. Discussion started: 13 November 2026
© Author(s) 2026. CC BY 4.0 License.

much lower mixing ratios in the mid-latitudinal lower stratosphere in autumn – unless a significant fraction of the air had recently experienced fast transport from a strong source region for both gases, as is the case for the ASMA. This matter will be examined further in Section 3.3 while temporal trends will be revisited in a more quantitative way in Section 3.4. Curtain plots for all remaining species can be found in the supplement. This includes perchloroethylene (C_2Cl_4), which is the third Cl-VSLS in our study. Mixing ratios of C_2Cl_4 are much lower than those of CH_2Cl_2 and $CHCl_3$, ranging from 0.12 to 1.2 ppt near the tropopause (> 210 ppt CFC-11). This, and the corresponding faster decrease with increasing altitude, is in line with expectations due to the much shorter lifetime (local and global) of this species. It is evidently the least relevant Cl-VSLS contributor to stratospheric chlorine here by some margin and therefore given less emphasis.

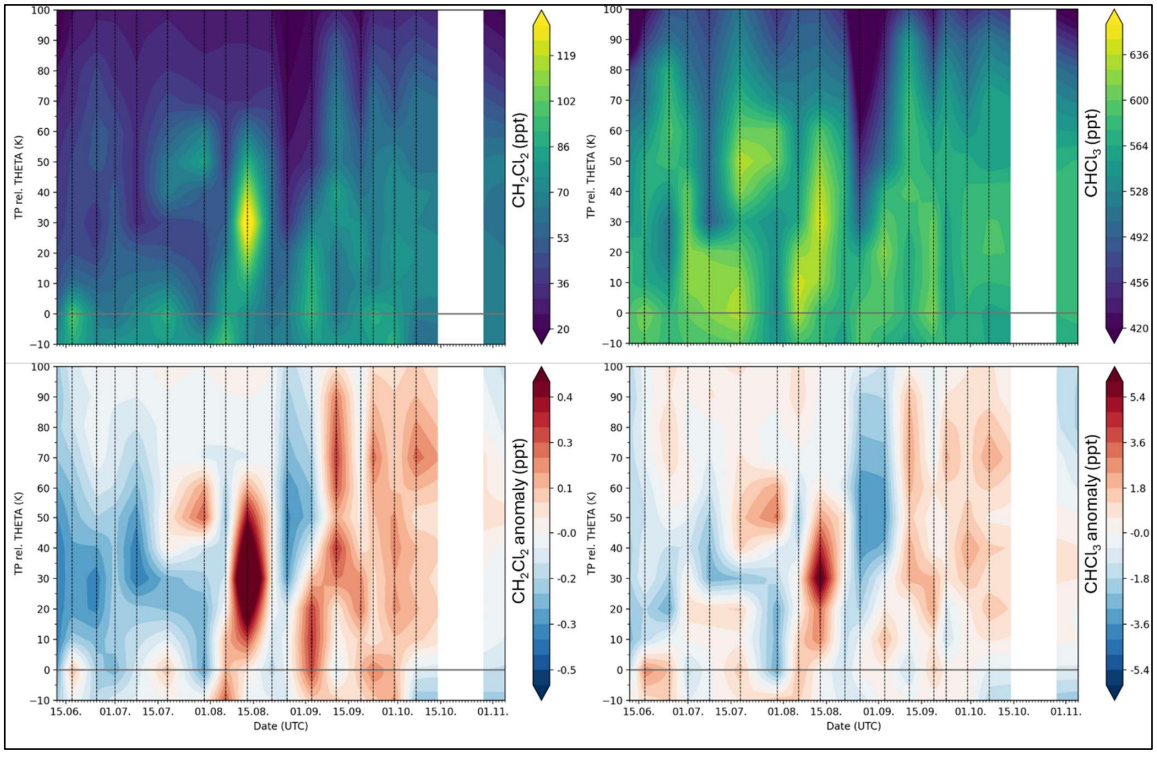


Figure 4 Same as in Fig. 3 but for CH_2Cl_2 and $CHCl_3$ (upper half) and, in addition, plotted as anomaly against the overall campaign average mixing ratio (lower half). For the anomalies, first a regular grid was created through interpolation from -10 to 180 K (tropopause-relative), then averaging was carried out over all 10-K and 1-day bins (equal to altitude ranges of -2 to 7.6 km in 0.4-km and 1-day bins).

https://doi.org/10.5194/egusphere-2026-6733
Preprint. Discussion started: 13 November 2026
© Author(s) 2026. CC BY 4.0 License.

3.2 Ozone and water vapor

Fig. 5 shows the corresponding data set for ozone and water vapour. As would be expected from an increasing influence of tropospheric air masses in the lower stratosphere towards autumn, ozone shows a tendency to lower mixing ratios. Given that these data originate from a different sensor package flown on a separately launched balloon, it is reassuring to be able to distinguish very similar patterns in the trace gas anomalies. For example, the previously mentioned mixing ratio enhancement event on 13th August exhibits low ozone across the same altitude range. Similarly, the air masses descending from higher up in the stratosphere on 26th August show high ozone at ~30-100 K above the tropopause, i.e., exactly where low halocarbon mixing ratios are being observed (Fig. 2 and 3). Importantly, O_3 is a very good tracer for stratospheric air, but far less specific for the determination of the exact source region of low-O_3 air in the troposphere; though in the context of the ASMA, low ozone has been found to be a good indicator for marine air that has been uplifted by tropical cyclones (Li et al., 2020 and 2021; Vogel et al., 2026). Still, the unique combination of a range of gases with very different source and sink distributions in this data set is therefore a major advantage for the analysis conducted here.

For water vapour, the patterns in the curtain plot (Fig. 5) are somewhat more complex. This is due to multiple distinctive properties of this gas, including, a) it being condensable with stratospheric mixing ratios therefore being predominantly governed by tropopause temperatures, b) potential influence from a range of source (different types of convection, isentropic transport, ice crystal sublimation, methane oxidation) and sink (condensation/resublimation/dehydration) processes, and c) an enormous vertical concentration gradient of several orders of magnitude across the tropopause.

At altitudes of approximately 2 km or higher above the tropopause, a weak negative correlation is observed (see also Figs. S4, S10, and S11) between water vapor and ozone, whereas the two trace gases show virtually no correlation around the tropopause. This indicates that different transport mechanisms are responsible for the two regimes in the lower stratosphere, reflecting the well-known layers ExTL, background LMS, and deeper stratosphere as described in 3.1. Interestingly, the strongest positive LMS anomaly in water on 11th and 19th September coincides with a positive anomaly in short-lived chlorinated compounds, suggesting that the Asian monsoon can be a source of water vapor in the lowermost stratosphere, in line with findings from previous studies (e.g., Rolf et al., 2018).

https://doi.org/10.5194/egusphere-2026-6733
Preprint. Discussion started: 13 November 2026
© Author(s) 2026. CC BY 4.0 License.

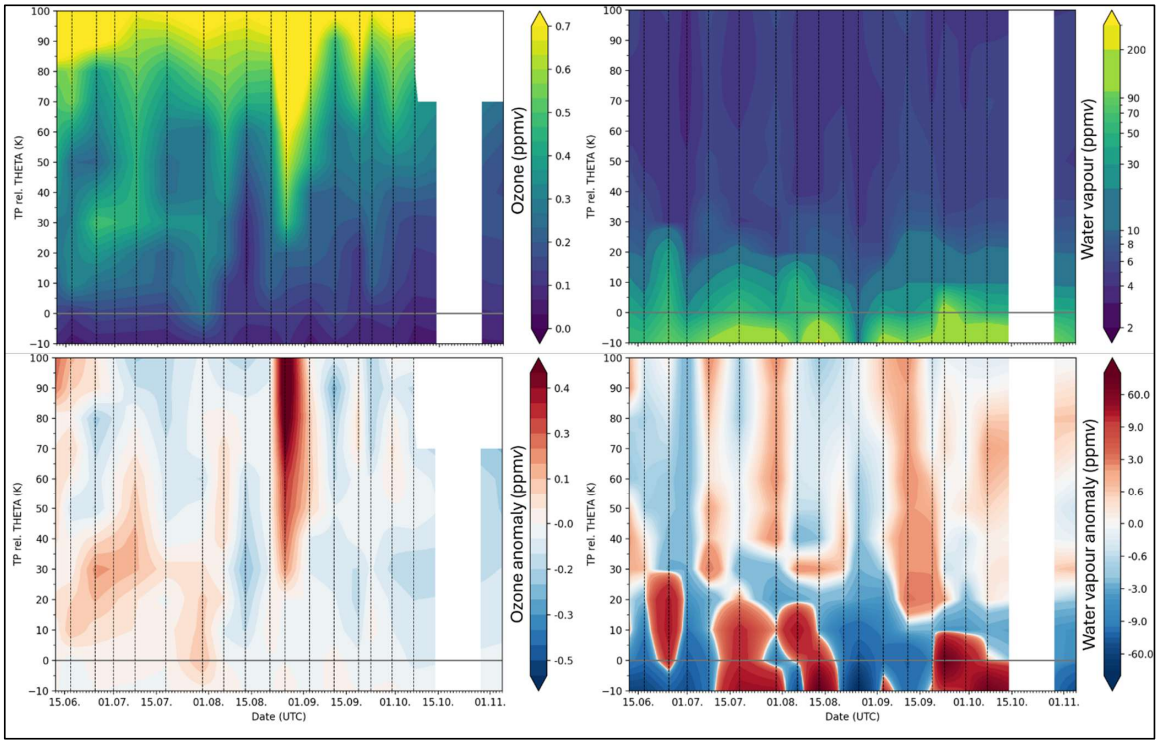


Figure 5 The same as in Fig. 4 but for ozone and water vapour.

3.3 Air mass origins

To investigate the origin of the enhanced mixing ratios observed for multiple halogenated species in late summer and autumn, three-dimensional global simulations were performed with the ERA-5 reanalysis-driven CLaMS model including surface-origin tracers (see 2.3). The upper two panels in Fig. 6 show curtain plots for the SA and the WP tracer as interpolated onto the balloon flight tracks. Particularly noticeable is that the monsoon origin region accounts for ~20-30% of lower stratospheric air above Europe in middle and late autumn, with the WP region less prominent but still ranging from ~10-15%. Both origin region plots show remarkable similarity with the patterns observed for the halogenated trace gases. Of course, this also means that they are very similar to each other. Air masses with different chemical compositions from SA and WP, mainly from tropical cyclones, can be mixed in filaments that are separated at the eastern flank from the ASMA (Vogel et al., 2026). Subsequently, these filaments can be transported further into the northern ExLS (Vogel et al., 2016). A direct assignment of the enhanced halocarbon mixing ratios to one or both regions or their sub-regions is beyond the scope of this work. It is however well known that many of the observed gases have strong anthropogenic emissions in China and, to a lesser degree, other countries in East and South Asia (e.g., SF_6, HFC-125, CH_2Cl_2, $CHCl_3$; Claxton et al., 2019; Laube and

https://doi.org/10.5194/egusphere-2026-6733
Preprint. Discussion started: 13 November 2026
© Author(s) 2026. CC BY 4.0 License.

Tegtmeier, 2023; Vojta et al., 2024; Zhang et al., 2026). Therefore, the far likelier pollution source of the two origin regions is the SA one as it encompasses much of continental East and South Asia.

In addition, the lower two panels of Fig. 6 show the full model output for the SA and WP tracer, averaged over a large area above the launch location in Jülich (50-60 °N and 0-12 °E), with a temporal resolution of 24 hours. In general, the temporal sampling of the BAMBI campaign (~1 week) yields good agreement with the 24-hour model output. However, individual filaments (e.g. on 13th August) appear less pronounced, reflecting the transport time of filaments which is not fully resolved at the campaign's weekly time resolution. Overall, the sampling from the BAMBI campaign appears to have captured a representative picture of this region.

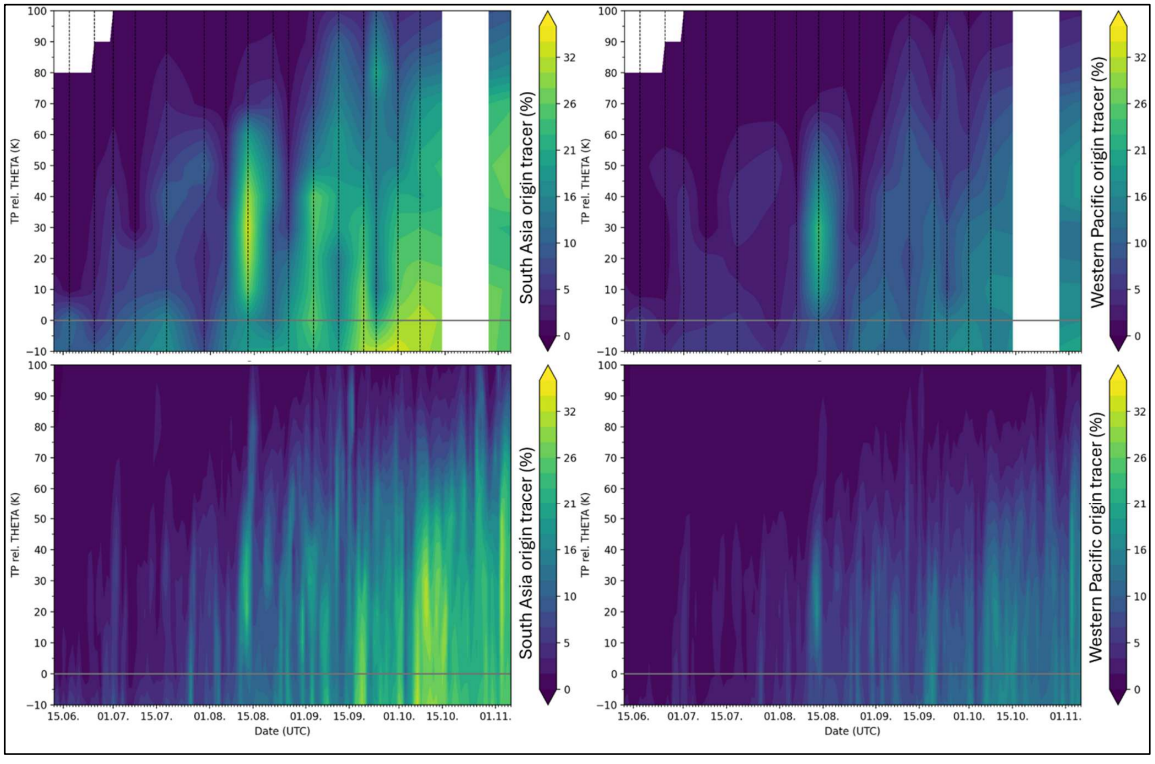


Figure 6 The top panels show the same as in Fig. 3 but for two model-based region-origin tracers, i.e., SA and the adjacent WP, both derived from matching model data to balloon flight coordinates. The lower two panels are the complete model data for the entire region from 50-60 °N and 0-12 °E. The corresponding sub-regions included in SA and WP can be found in Fig. 1.

https://doi.org/10.5194/egusphere-2026-6733
Preprint. Discussion started: 13 November 2026
© Author(s) 2026. CC BY 4.0 License.

3.4 Temporal UTLS composition evolution and impact on the equivalent chlorine budget

As one of the main aims of this study is to determine the evolution of the "background" lower and lowermost stratospheric composition in the NH over summer and autumn, it is important to remove air masses that are not well mixed before attempting such an analysis. Air that has recently entered the stratosphere is typically characterised by a differing potential vorticity (PV, e.g., Danielsen, 1968). We here use the PV calculated from ERA-5 (interpolated onto the flight paths) to exclude filaments separated from the ASMA as, e.g., encountered during the flight on 13th August. The data is first subdivided into four 2 km-wide altitude layers in the vicinity of the tropopause and the average mole fractions in those layers are derived for each flight. All points outside the one standard deviation PV range for a respective altitude layer are then removed. Fig. 7 and 8 show the resulting time series for all eight halogenated species alongside the ground-based observations (see 2.4). Stratospheric "background" abundances are mostly somewhat lower at higher altitudes as a result of long-range transport-related "temporal offsets" as well as, in the case of the species with significant sinks along the transport paths, chemical decay.

In terms of short-term trends, balloon-based ones in the layer below the tropopause are most consistent with the ground-based ones, especially for longer-lived species such as SF_6, HFC-125, or CFC-11. Above the tropopause there is however more of a disconnect as mole fraction increases in the region up to 6 km above the tropopause are more positive than the ground-based ones. This tendency is most pronounced 2-4 km above the tropopause, with increases of up to four times higher than those observed near ground over the same period (Table 2). Especially noteworthy here is CH_2Cl_2, which almost reaches lower tropospheric abundances at these high altitudes in late September and early October. For the other two Cl-VSLSs, $CHCl_3$ and C_2Cl_4, the near-tropopause abundances are distinctly lower, likely owing to their faster chemical decay in the atmosphere (Burkholder and Hodnebrog, 2023). The comparison of ground-based with balloon-based data over the same time windows has some limitations. Air typically needs several months to travel from the ground to the lower stratosphere, though these transport times can be only weeks in the case of air entering through the ASMA (e.g., Wetzel et al., 2021, Lauther et al., 2022). This can however not easily be accounted for here, as transport tracers like SF_6 and HFC-125 are clearly also directly impacted by the monsoon influence (Fig. 7). These gases also have strong emissions in the ASMA input regions and are therefore potentially entering the stratosphere with an unknown mixing ratio enhancement.

For CH_2Cl_2, we would expect the decreasing near-ground mole fractions from the first campaign half to be reflected in the lower stratosphere in the second campaign half – but this is not the case, highlighting the impact of the fast monsoon-based transport pathway. It is worth keeping in mind that the levels of Cl-VSLSs observed here are mostly much lower than those found in the vicinity of the ASMA (see discussion and references in Section 1) – yet also much less variable, indicating that the endeavour of this study to predominantly sample "background" stratospheric air has been successful.

https://doi.org/10.5194/egusphere-2026-6733
Preprint. Discussion started: 13 November 2026
© Author(s) 2026. CC BY 4.0 License.

Over much of the campaign, the observed pronounced mole fraction increases correlate well with each other as well as the model-based fraction of monsoon-related air (Figures 3-6, Figures S6-S11). Only in the last month we find that, while very long-lived species like SF_6 exhibit stable or further increasing mole fractions, the shorter-lived species like CH_2Cl_2 show indications of beginning to decrease (Figure 7 and 8). This decrease is likely related to the combined effect of a) further input from the monsoon having faded, and b) chemical ageing of the air inside the stratosphere. A potential alternative explanation would be monsoon air reaching the lower stratosphere via the tropics (i.e. through the lower branch of the Brewer-Dobson circulation). However, this would also decrease mole fractions of species with sinks in the lower tropical stratosphere and/or TTL such as CFC-11 and H-1211, which is only observed in the highest layer investigated here, 4-6 km above the tropopause.

Alongside the observational data, Figures 7 and 8 show the mole fractions from the model study of Liang et al., 2025 (where available). The two datasets agree reasonably well for most species, the most notable exceptions being HCFC-22 and CH_2Cl_2. Liang et al. appear to significantly and consistently overestimate the amount of HCFC-22 entering the stratosphere by about 30 ppt. However, the reference period of the Liang et al. study is 2020-2022, i.e., several years earlier than the BAMBI campaign. The discrepancy might therefore be, at least in part, related to the decrease in global HCFC-22 emissions in recent years (Laube and Tegtmeier, 2023; Zhang et al., 2026). In the case of CH_2Cl_2, the modelled and observed abundances in the lower stratosphere above Europe are similar to each other at the beginning of the campaign period. However, observations show a much more pronounced increase over time, resulting in a difference of almost 30 ppt (>50 %) by early October. This might well be partly related to global emissions of CH_2Cl_2 having continued to increase, especially in China as one of the main monsoon input regions (Zhang et al., 2026); on the other hand, the transport pathway through the ASMA might also be more effective than previously thought.

To evaluate the potential impacts on the ozone layer, we derive the organic equivalent chlorine (ECl) contained in the six ozone-depleting substances in this study (Table 2). ECl reached 1194 ± 82 ppt in October in the region 2-4 km above the tropopause, with a contribution of 185 ± 29 ppt from the three Cl-VSLS. This represents an increase over the campaign period of 161 ± 21 ppt, of which about half (85 ± 12 ppt) are from Cl-VSLS. This is much higher than the enhancement range estimated from observations above the central ASMA by Adcock et al. (2021), i.e. 0.3–34.9 ppt of ECl – but based on of a wider range of ODSs, and for the entire NH lower stratosphere. Comparing to the model study of Liang et al. (2025) is much more direct as the latitudes and altitudes can be narrowed down in the model data. They find a similar absolute amount of 1146 ± 80 ppt for five of the six ODSs (with the C_2Cl_4 contribution in this study's estimate essentially negligible), but with a smaller Cl-VSLS contribution of 107 ± 32 ppt. Again, the reference period of the Liang et al. study is 2020-2022. Since then, global abundances of both CFC-11 and H-1211 have decreased considerably (Western et al., 2025) while those of CH_2Cl_2 have only increased slightly (Western et al., 2025; Zhang et al., 2026). Therefore, the total equivalent chlorine during the BAMBI campaign would be expected to be somewhat lower, not higher. More importantly (and also more quantitatively), the observed Cl-VSLS abundance expressed as equivalent chlorine is on average 1.7 times higher than the

https://doi.org/10.5194/egusphere-2026-6733
Preprint. Discussion started: 13 November 2026
© Author(s) 2026. CC BY 4.0 License.

previously modelled one; with Liang et al. already concluding that the Asian Summer Monsoon is the dominant stratospheric entry pathway for these substances.

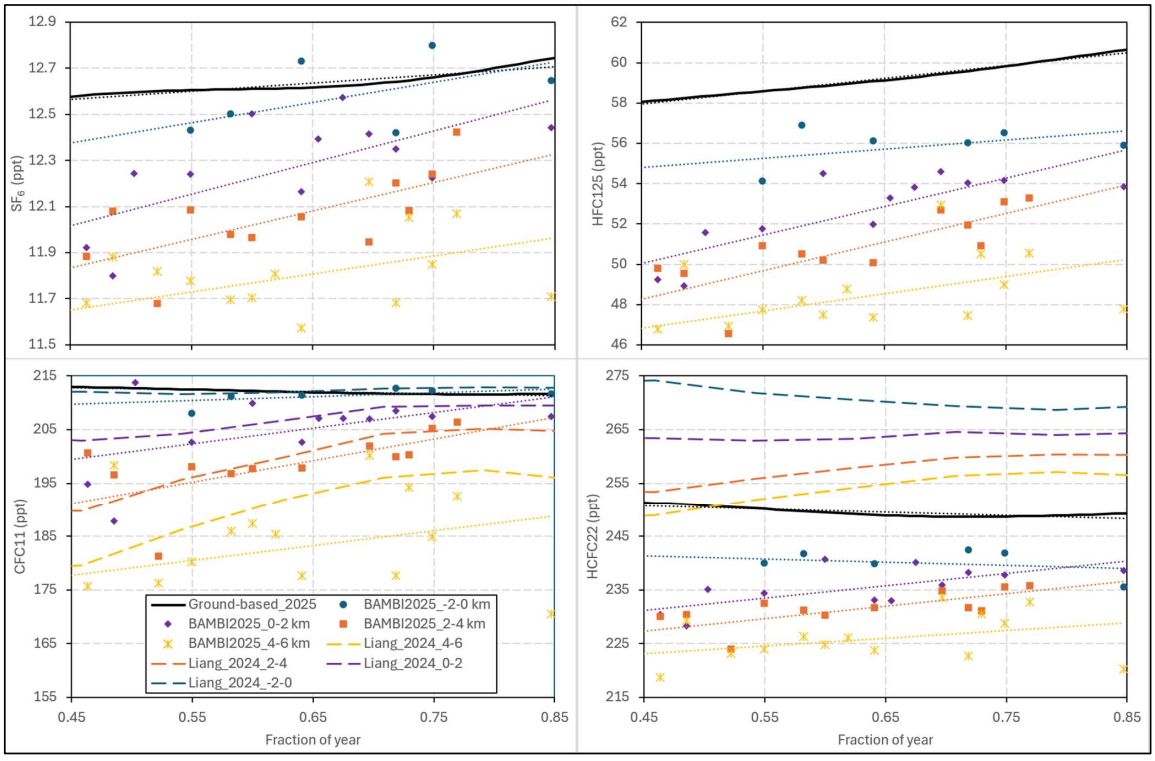


Figure 7 Time series (expressed as fractions of the year) of mole fractions of SF_6, HFC-125, CFC-11, and HCFC-22 observed during the BAMBI campaign a) at the Taunus Observatory near Frankfurt (Main) in Germany (ground-based, black lines) as well as b) from the balloon flights, averaged over various altitude layers in the vicinity of the tropopause (symbols). Dotted lines are derived as linear trends through the respective data over the 5-month campaign period, while dashed lines are model-based estimates of mole fractions in the same near-tropopause layers from the study of Liang et al., 2025 (zonal mean values averaged over a latitude range of 50-52 °N; only available for CFC-11 and HCFC-22).

https://doi.org/10.5194/egusphere-2026-6733
Preprint. Discussion started: 13 November 2026
© Author(s) 2026. CC BY 4.0 License.

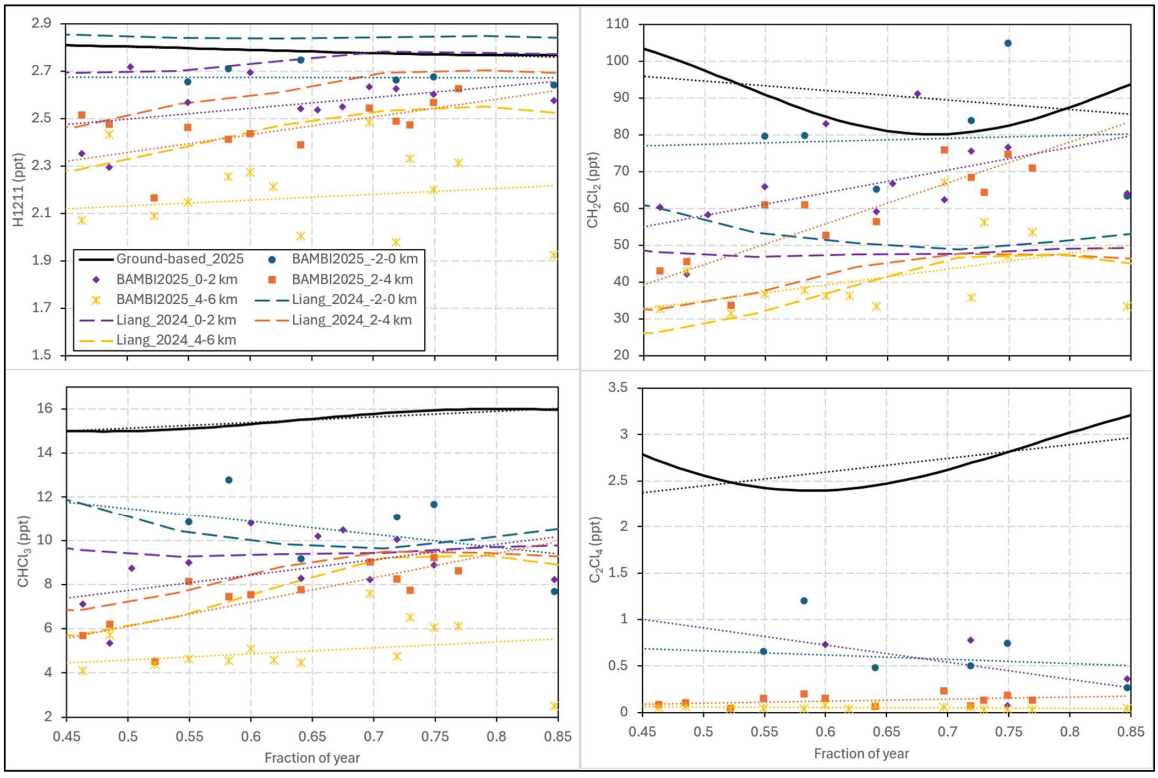


Figure 8 The same as in Figure 7, but for H-1211, CH_2Cl_2, $CHCl_3$, and C_2Cl_4. Note that for CH_2Cl_2 and $CHCl_3$ the ground-based data as well as that from Liang et al., 2025 have been converted to NOAA calibration scales (Table 1) to correct for significant calibration-related differences between the two major networks (AGAGE and NOAA GML; Laube and Tegtmeier, 2023). This conversion was carried out following a recent lab calibration intercomparison exercise (Laube et al., 2025).

Table 2 Mole fraction changes estimated from linear regressions during the BAMBI 2025 campaign period. Data shown originates from observations at the Taunus Observatory near Frankfurt (Main) in Germany (ground-based) as well as in various altitude layers in the vicinity of the tropopause (TP). The second-to-last column represents the corresponding change in organic equivalent chlorine (ECl_{org}) contained in those trace gases in the layer between 2 and 4 km above the tropopause. Shown next to it are the model-derived average ECl_{org} values in the same region from Liang et al., 2025 (note that these correspond to different base years, i.e., 2020-2022). Uncertainty ranges are derived as one standard deviation of the slope of the regression line, and therefore mainly represent atmospheric variability (including seasonal trend variability). For all balloon-based data, samples with a high potential vorticity (model-based) were filtered out to minimise the influence of recently displaced air that is not representative of large-scale UTLS composition (see section 3.4). All species are reported on consistent calibration scales (see Table 1).

Trace gas	Mole fraction change during BAMBI campaign (ppt, PV-filtered):	ΔECl_{org}	ΔECl_{org_model}

https://doi.org/10.5194/egusphere-2026-6733
Preprint. Discussion started: 13 November 2026
© Author(s) 2026. CC BY 4.0 License.

	Ground-level	TP_{rel} -2-0 km	TP_{rel} 0-2 km	TP_{rel} 2-4 km	TP_{rel} 4-6 km	(2-4 km)	(2-4 km)[a]
SF_6	0.14 ± 0.16	0.35 ± 0.18	0.55 ± 0.17	0.49 ± 0.14	0.31 ± 0.17	0	0
HFC-125	2.6 ± 0.9	1.8 ± 1.2	5.7 ± 1.1	5.7 ± 1.2	3.4 ± 1.7	0	0
CFC-11	-1.5 ± - 0.3	2.8 ± 1.6	12 ± 6	16 ± 5	11 ± 11	48 ± 16	44 ± 9
HCFC-22	-2.5 ± 0.6	-2.3 ± 2.9	9.2 ± 2.8	9.2 ± 2.5	5.8 ± 3.9	9.2 ± 2.5	6.9 ± 1.2
H-1211	-0.05 ± 0.02	0.00 ± 0.14	0.18 ± 0.27	0.30 ± 0.29	0.10 ± 0.05	18 ± 7[b]	14 ± 3[b]
CH_2Cl_2	-12 ± 7[c,d]	3 ± 15[c]	20 ± 10[c]	37 ± 6[c]	14 ± 7[c]	74 ± 12[c]	25 ± 7[c,d]
$CHCl_3$	1.2 ± 0.8[c,d]	-2.0 ± 1.6	2.3 ± 1.2[c]	3.6 ± 0.7[c]	0.9 ± 1.0[c]	11 ± 2[c]	6.6 ± 1.8[c,d]
C_2Cl_4	0.6 ± 0.6	-0.2 ± 0.4	0.0 ± 0.1	0.1 ± 0.1	-0.02 ± 0.01	0.3 ± 0.2	-

[a]from Liang et al., 2025; [b]using an α factor of 60 for the higher ozone depletion efficiency of bromine (Laube and Tegtmeier, 2023); [c]Only derived over the first four months as abundances no longer follow the regression line during the last one; [d]Calibration scale-adjusted, see caption of Fig. 8 for details.

4 Conclusions and outlook

This study presents a unique observation-based dataset that allows insights into the distributions of ten trace gases in the sparsely sampled UTLS region and their evolution over a period of about 5 months during summer and autumn 2025 to analyse the impact of the Asian summer monsoon on the northern UTLS over Europe. All species were found to correlate with each other (Figs. 2, S6-S11), including ozone and water vapour (although for the latter the correlation is weaker due to its multiple sources, Figure S10). While the underlying balloon launches took place on an almost weekly basis during that period, the considerable variability in this atmospheric region warrants a note of caution regarding the representativity of the data (even after PV filtering), especially for the highly variable water vapour and Cl-VSLSs. However, the complementing model data suggests that the balloon-based data can capture the overall temporal evolution of the UTLS composition quite well (Fig. 6). In addition, while the multiple launches during the 2025 BAMBI campaign provide more than a snapshot of UTLS composition above Europe, interannual variability could not be captured. For the eight halogenated species, we find abundances that are largely consistent with regional ground-based observations, as well as with published model-based estimates of their UTLS distributions. There are however a few noteworthy exceptions. Firstly, the short-term trends of all eight species, as observed over the summer and into autumn, are distinctly more positive than the ground-based ones. This is particularly pronounced for CH_2Cl_2, with its chlorine content increasing by 74 ± 12 ppt in the lower stratosphere by early October, as compared to 25 ± 7 ppt from a recent model study that already highlighted the importance of the monsoon-based stratospheric entry pathway for Cl-VSLSs (Liang et al., 2025). It is also much higher than the observation-/model-based estimate of Adcock et al. (2021), who derived ASMA-originating enhancements of 0.3–34.9 ppt of Equivalent Chlorine (ECl) from a much wider range of compounds. Our study thus provides indications for this transport pathway still being underestimated, especially as additional evidence for the near-ground source regions of the enhanced abundances is provided

https://doi.org/10.5194/egusphere-2026-6733
Preprint. Discussion started: 13 November 2026
© Author(s) 2026. CC BY 4.0 License.

by a model-based surface-origin tracer. The Ozone Depletion Potentials (ODPs) of these species are, due their short atmospheric lifetimes, dependent on the emission region. As mentioned in the Introduction, Claxton et al. (2019) already found that for this reason Southeast Asian emissions can have up to a factor of 3 times greater potential to deplete stratospheric ozone than European ones. Judging from our observations, this is likely to still be an underestimate, supported by monsoon-related air fractions of up to ~30% (for the SA region) and ~15% (for WP) above Europe in autumn from the corresponding model runs. The Cl-VSLSs are likely to release much of their chlorine inside the stratosphere due to their short lifetimes. In contrast, the longer-lived species are not, as their main sink region is in the tropics, which has been largely bypassed by air entering the LMS through the Asian monsoon pathway; though how much of the longer-lived ODSs reach the tropical stratosphere via the monsoon anticyclone pathway is currently not well known.

Different implications arise from the observed enhanced abundances of the very long-lived species. SF_6 and HFC-125 have been extensively used to derive average stratospheric transit times, i.e., mean ages-of-air (e.g., Volk et al., 1996; Andrews et al., 2001; Boenisch et al., 2009; Leedham Elvidge et al., 2018; Laube et al., 2025). The lower stratosphere is known to be globally influenced by tropospheric air, especially in autumn. Recent age-of-air estimation methods have been taking this into account (e.g., Wagenhäuser et al., 2023; Ray et al., 2024). The increasing lower stratospheric mole fractions observed during BAMBI are however clearly associated with enhanced fractions of air that has entered the stratosphere through the ASMA (Figures 3 and 6, Figures S6-S11), i.e. from regions with strong emission sources of these gases. This raises the question of how much of a bias such a longitudinally asymmetric transport pathway containing an unquantified component of air "polluted" in these gases might cause in age-of-air estimates. Also, such pronounced mole fraction enhancements were not observed during an aircraft campaign in the vicinity of the central ASMA (Adcock et al., 2021). Consequently, other monsoon-related stratospheric entrance pathways, e.g., through the Eastern Asian Monsoon (EAM, Pan et al., 2024), might be of higher importance than previously thought. This is supported by the closer vicinity of major emission regions to the EAM, especially for those gases with the most pronounced increases observed in the lower stratosphere during the BAMBI campaign: SF_6, HFC-125, and CH_2Cl_2. However, quantitatively evaluating this mechanism as well as its impact on age of air estimates is beyond the scope of this study. The dataset is nevertheless suitable for contributing to such potential future investigations, e.g. via the validation of model- or satellite-based trace gas distributions (e.g., De Longueville et al., 2023). It also nicely demonstrates the observational capabilities that have become available using simple, cost-effective, weather balloon-based sensor packages.

Author contributions.

JCL, CR, AM, MG, and MIH contributed to the execution of the campaign and the operation of the instrumentation in the field and lab, including post-flight sample analysis. JCL, CR, AM, and MG contributed to data analysis and interpretation, whereas BV provided CLaMS model output including its interpretation, while AE and TW provided ground-based observational data. JCL drafted the manuscript, and all coauthors contributed to improving it.

https://doi.org/10.5194/egusphere-2026-6733
Preprint. Discussion started: 13 November 2026
© Author(s) 2026. CC BY 4.0 License.

Competing interests.

The authors also have no competing interests to declare.

Disclaimer.

Publisher's note: Copernicus Publications remains neutral with regard to jurisdictional claims made in the text, published maps, institutional affiliations, or any other geographical representation in this paper. While Copernicus Publications makes every effort to include appropriate place names, the final responsibility lies with the authors. Also, please note that this paper has not received English language copy-editing.

Special issue statement. This article is part of the special issue "The tropopause region in a changing atmosphere (TPChange) (ACP/AMT/GMD/WCD inter-journal SI)". It is not associated with a conference.

Acknowledgements.

We are extremely grateful for the support from the technical staff before, during, and after the campaign, especially from Wilhelm Steffes, Lucia Iwan, Sena Sarioglu, Markus Retzlaff, Nicole Spelten, Anne Richter, Andreas Sitnikov, Jochen Barthel, and Vicheith Tan (all FZJ). Also invaluable was the support from many more colleagues during various flights and recoveries, especially during the summer holiday season. We cannot name everyone but are highlighting Julia Finke and Armin Afchine here. We acknowledge the work of the NOAA Global Monitoring Laboratory as well as the AGAGE network for providing consistent calibration scales of multiple trace gases.

Financial support.

The balloon soundings were partly supported by the Helmholtz Association in the framework of the MOSES (Modular Observation Solutions for Earth Systems) project. The study was also partly funded by the Deutsche Forschungsgemeinschaft (DFG, German Research Foundation) as part of TPChange – TRR 301 TPChange – Project-ID 428312742. We thank the European Centre for Medium-Range Weather Forecasts (ECMWF) for providing the ERA5 reanalyses and the Jülich Supercomputing Centre (JSC; Research Centre Jülich, Germany) for the computing time on the supercomputer JUWELS (project CLaMS-ESM) and for the storage resources. The measurements at Taunus Observatory were financed in part by the European Union's Horizon Europe Research and Innovation programme under HORIZON-CL5-2022-D1-02 Grant Agreement No 101081430 – PARIS. The Medusa instrument at Taunus Observatory was funded by the German Federal Ministry of Education and Research through the German component of ACTRIS (Aerosol, Clouds and Trace Gases Research Infrastructure) under grant 01LK2001I.

https://doi.org/10.5194/egusphere-2026-6733
Preprint. Discussion started: 13 November 2026
© Author(s) 2026. CC BY 4.0 License.

References

Adcock, K. E., Fraser, P. J., Hall, B. D., Langenfelds, R. L., Lee, G., Montzka, S. A., Oram, D. E., Röckmann, T., Stroh, F., Sturges, W. T., Vogel, B., and Laube, J. C.: Aircraft-Based Observations of Ozone-Depleting Substances in the Upper Troposphere and Lower Stratosphere in and Above the Asian Summer Monsoon, J. Geophys. Res., 126, e2020JD033137, https://doi.org/10.1029/2020JD033137, 2021.

Andrews, A. E., Boering, K. A., Daube, B. C.,Wofsy, S. C., Loewenstein, M., Jost, H., Podolske, J. R.,Webster, C. R., Herman, R. L., Scott, D. C., Flesch, G. J., Moyer, E. J., Elkins, J. W., Dutton, G. S., Hurst, D. F., Moore, F. L., Ray, E. A., Romashkin, P. A., and Strahan, S. E.: Mean ages of stratospheric air derived from in situ observations of CO2, CH4, and N2O, J. Geophys. Res.-Atmos., 106, 32295–32314, https://doi.org/10.1029/2001JD000465, 2001.

Bönisch, H., Engel, A., Curtius, J., Birner, Th., and Hoor, P.: Quantifying transport into the lowermost stratosphere using simultaneous in-situ measurements of SF6 and CO2, Atmos. Chem. Phys.,9, 5905–5919, doi:10.5194/acp-9-5905-2009, 2009.

Burkholder, J. B. and Hodnebrog, Ø.: Summary of Abundances, Lifetimes, ODPs, REs, GWPs, and GTPs, in: Scientific Assessment of Ozone Depletion: 2022, World Meteorological Organization, Geneva, Switzerland, ISBN 978-9914-733-97-6, 2023.

Claxton, T., Hossaini, R., Wild, O., Chipperfield, M. P., and Wilson, C.: On the Regional and Seasonal Ozone Depletion Potential of Chlorinated Very Short-Lived Substances, Geophys. Res. Lett., 46, 5489–5498, https://doi.org/10.1029/2018GL081455, 2019.

Danielsen, E. F.: Stratospheric-Tropospheric Exchange Based on Radioactivity, Ozone and Potential Vorticity, Journal of Atmospheric Sciences, 25, 502–518, https://doi.org/10.1175/1520-0469(1968)025<0502:STEBOR>2.0.CO;2, 1968.

De Longueville, H., Clarisse, L., Whitburn, S., Clerbaux, C., Lecomte, G., and Coheur, P.: Atmospheric trends of long-lived halogenated gases derived from 15 years of IASI measurements, J. Quant. Spectrosc. Radiat. Transf., 311, 108755, doi: 10.1016/j.jqsrt.2023.10875 , 2023.

Dirksen, R. J., Bodeker, G. E., Thorne, P. W., Merlone, A., Reale, T., Wang, J., Hurst, D. F., Demoz, B. B., Gardiner, T. D., Ingleby, B., Sommer, M., von Rohden, C., and Leblanc, T.: Managing the transition from Vaisala RS92 to RS41 radiosondes

https://doi.org/10.5194/egusphere-2026-6733
Preprint. Discussion started: 13 November 2026
© Author(s) 2026. CC BY 4.0 License.



within the Global Climate Observing System Reference Upper-Air Network (GRUAN): a progress report, Geosci. Instrum. Method. Data Syst., 9, 337–355, https://doi.org/10.5194/gi-9-337-2020, 2020.

Dubé, K., Tegtmeier, S., Bourassa, A., Laube, J. C., Engel, A., Saunders, L. N., Walker, K. A., Hossaini, R., and Bednarz, E. M.: Chlorinated very short-lived substances offset the long-term reduction of inorganic stratospheric chlorine, Commun. Earth Environ., 6, 487, https://doi.org/10.1038/s43247-025-02478-9, 2025.

Fang, X., Park, S., Saito, T., Tunnicliffe, R., Ganesan, A. L., Rigby, M., Li, S., Yokouchi, Y., Fraser, P. J., Harth, C. M., Krummel, P. B., Mühle, J., O'Doherty, S., Salameh, P. K., Simmonds, P. G., Weiss, R. F., Young, D., Lunt, M. F., Manning, A. J., Gressent, A., and Prinn, R. G.: Rapid increase in ozone-depleting chloroform emissions from China, Nat. Geosci., 12, 89–93, https://doi.org/10.1038/s41561-018-0278-2, 2019.

Geldenhuys, M., Blazaki, K., Afchine, A., Cereceda, F., Grooß, J.-U., Hegglin, M. I., Kloss, C., Kuhn, T., Labuschagne, C., Labuschagne, P., Laube, J. C., Machinini, T., Mkololo, T., Renard, J.-B., Rolf, C., Steffes, W., Stopford, C., Riese., M.: BIANKA: A Balloon Field Campaign to Study Climate Change Uncertainties, Extended Abstract in: Proceedings of the 38th Annual Conference of the South African Society for Atmospheric Sciences, First Edition, ISBN: 978-1-0370-1666-0, Potchefstroom, South Africa, 2024.

Gettelman, A., Hoor, P., Pan, L. L., Randel, W. J., Hegglin, M. I., and Birner, T.: The Extratropical Upper Troposphere And Lower Stratosphere, Rev. Geophys., 49, RG3003, https://doi.org/10.1029/2011RG000355, 2011.

Graßl, S., Ritter, C., Tritscher, I., and Vogel, B.: Does the Asian summer monsoon play a role in the stratospheric aerosol budget of the Arctic?, Atmos. Chem. Phys., 24, 7535–7557, https://doi.org/10.5194/acp-24-7535-2024, 2024.

Hegglin, M. I. and Shepherd, T. G.: O3-N2O correlations from the Atmospheric Chemistry Experiment: Revisiting a diagnostic of transport and chemistry in the stratosphere, J. Geophys. Res., 112, D19301, https://doi.org/10.1029/2006JD008281, 2007.

Hegglin, M. I., Boone, C. D., Manney, G. L., and Walker, K. A.: A global view of the extratropical tropopause transition layer from Atmospheric Chemistry Experiment Fourier Transform Spectrometer O3, H2O, and CO, J. Geophys. Res., 114, D00B11, doi:10.1029/2008JD009984, 2009.

Hersbach, H., Bell, B., Berrisford, P., Hirahara, S., Horanyi, A., Munoz-Sabater, J., Nicolas, J., Peubey, C., Radu, R., Schepers, D., Simmons, A., Soci, C., Abdalla, S., Abellan, X., Balsamo, G., Bechtold, P., Biavati, G., Bidlot, J., Bonavita,

https://doi.org/10.5194/egusphere-2026-6733
Preprint. Discussion started: 13 November 2026
© Author(s) 2026. CC BY 4.0 License.



M., De Chiara, G., Dahlgren, P., Dee, D., Diamantakis, M., Dragani, R., Flemming, J., Forbes, R., Fuentes, M., Geer, A., Haimberger, L., Healy, S., Hogan, R. J., Hólm, E., Janiskova, M., Keeley, S., Laloyaux, P., Lopez, P., Lupu, C., Radnoti, G., de Rosnay, P., Rozum, I., Vamborg, F., Villaume, S., and Thepaut, J.-N.: The ERA5 global reanalysis, Q. J. Roy. Meteorol. Soc., 146, 1999–2049, https://doi.org/10.1002/qj.3803, 2020.

Hossaini, R., Atlas, E., Dhomse, S. S., Chipperfield, M. P., Bernath, P. F., Fernando, A. M., Mühle, J., Leeson, A. A., Montzka, S. A., Feng, W., Harrison, J. J., Krummel, P., Vollmer, M. K., Reimann, S., O'Doherty, S., Young, D., Maione, M., Arduini, J., and Lunder, C. R.: Recent Trends in Stratospheric Chlorine From Very Short-Lived Substances, J. Geophys. Res.-Atmos., 124, 2318–2335, https://doi.org/10.1029/2018JD029400, 2019.

Jesswein, M., Lauther, V., Emig, N., Hoor, P., Keber, T., Lachnitt, H.-C., Ort, L., Schuck, T., Strobel, J., Van Luijt, R., Volk, C. M., Weyland, F., and Engel, A.: Tracing elevated abundance of CH2Cl2 in the subarctic upper troposphere to the Asian Summer Monsoon, Atmos. Chem. Phys., 25, 8107–8126, https://doi.org/10.5194/acp-25-8107-2025, 2025.

Jorge, T., Brunamonti, S., Poltera, Y., Wienhold, F. G., Luo, B. P., Oelsner, P., Hanumanthu, S., Singh, B. B., Körner, S., Dirksen, R., Naja, M., Fadnavis, S., and Peter, T.: Understanding balloon-borne frost point hygrometer measurements after contamination by mixed-phase clouds, Atmos. Meas. Tech., 14, 239–268, https://doi.org/10.5194/amt-14-239-2021, 2021.

Karion, A., Sweeney, C., Tans, P., and Newberger, T.: AirCore: An Innovative Atmospheric Sampling System, J. Atmos. Ocean. Tech., 27, 1839–1853, https://doi.org/10.1175/2010JTECHA1448.1, 2010.

Khaykin, S. M., Godin-Beekmann, S., Keckhut, P., Hauchecorne, A., Jumelet, J., Vernier, J.-P., Bourassa, A., Degenstein, D. A., Rieger, L. A., Bingen, C., Vanhellemont, F., Robert, C., DeLand, M., and Bhartia, P. K.: Variability and evolution of the midlatitude stratospheric aerosol budget from 22 years of ground-based lidar and satellite observations, Atmos. Chem. Phys., 17, 1829–1845, https://doi.org/10.5194/acp-17-1829-2017, 2017.

Khordakova, D., Rolf, C., Grooß, J.-U., Müller, R., Konopka, P., Wieser, A., Krämer, M., and Riese, M.: A case study on the impact of severe convective storms on the water vapor mixing ratio in the lower mid-latitude stratosphere observed in 2019 over Europe, Atmos. Chem. Phys., 22, 1059–1079, https://doi.org/10.5194/acp-22-1059-2022, 2022.

Laube, J. C., Engel, A., Bönisch, H., Möbius, T., Worton, D. R., Sturges, W. T., Grunow, K., and Schmidt, U.: Contribution of very short-lived organic substances to stratospheric chlorine and bromine in the tropics – a case study, Atmos. Chem. Phys., 8, 7325–7334, https://doi.org/10.5194/acp-8-7325-2008, 2008.

https://doi.org/10.5194/egusphere-2026-6733
Preprint. Discussion started: 13 November 2026
© Author(s) 2026. CC BY 4.0 License.



570 Laube, J. C., Leedham Elvidge, E. C., Adcock, K. E., Baier, B., Brenninkmeijer, C. A. M., Chen, H., Droste, E. S., Grooß, J.-U., Heikkinen, P., Hind, A. J., Kivi, R., Lojko, A., Montzka, S. A., Oram, D. E., Randall, S., Röckmann, T., Sturges, W. T., Sweeney, C., Thomas, M., Tuffnell, E., and Ploeger, F.: Investigating stratospheric changes between 2009 and 2018 with halogenated trace gas data from aircraft, AirCores, and a global model focusing on CFC-11, Atmos. Chem. Phys., 20, 9771–9782, https://doi.org/10.5194/acp-20-9771-2020, 2020.

575

Laube, J. C. and Tegtmeier: Update on Ozone-Depleting Substances (ODSs) and Other Gases of Interest to the Montreal Protocol, in: Scientific Assessment of Ozone Depletion: 2022, GAW Report No. 278, World Meteorological Organization, Geneva, Switzerland, ISBN 978-9914-733-97-6, 2023.

580 Laube, J. C., Schuck, T. J., Baartman, S., Chen, H., Geldenhuys, M., van Heuven, S., Keber, T., Popa, M. E., Tuffnell, E., Voet, F., Vogel, B., Wagenhäuser, T., Zanchetta, A., and Engel, A.: Vertical distribution of halogenated trace gases in the summer Arctic stratosphere based on two independent air sampling methods, Atmos. Meas. Tech., 18, 4087–4102, https://doi.org/10.5194/amt-18-4087-2025, 2025.

585 Lauther, V., Vogel, B., Wintel, J., Rau, A., Hoor, P., Bense, V., Müller, R., and Volk, C. M.: In situ observations of CH2Cl2 and CHCl3 show efficient transport pathways for very short-lived species into the lower stratosphere via the Asian and the North American summer monsoon, Atmos. Chem. Phys., 22, 2049–2077, https://doi.org/10.5194/acp-22-2049-2022, 2022.

Leedham Elvidge, E. C., Bönisch, H., Brenninkmeijer, C. A. M., Engel, A., Fraser, P. J., Gallacher, E., Langenfelds, R.,
590 Mühle, J., Oram, D. E., Ray, E. A., Ridley, A. R., Röckmann, T., Sturges,W. T.,Weiss, R. F., and Laube, J. C.: Evaluation of stratospheric age of air from CF4, C2F6, C3F8, CHF3, HFC-125, HFC-227ea and SF6; implications for the calculations of halocarbon lifetimes, fractional release factors and ozone depletion potentials, Atmos. Chem. Phys., 18, 3369–3385, https://doi.org/10.5194/acp-18-3369-2018, 2018.

595 Li, D., Vogel, B., Müller, R., Bian, J., Günther, G., Ploeger, F., Li, Q., Zhang, J., Bai, Z., Vömel, H., and Riese, M.: Dehydration and low ozone in the tropopause layer over the Asian monsoon caused by tropical cyclones: Lagrangian transport calculations using ERA-Interim and ERA5 reanalysis data, Atmos. Chem. Phys., 20, 4133–4152, https://doi.org/10.5194/acp-20-4133-2020, URL https://www.atmos-chem-phys.net/20/4133/2020/, 2020.

600 Li, D., Vogel, B., Müller, R., Bian, J., Günther, G., and Riese, M.: Tropical Cyclones Reduce Ozone in the Tropopause Region Over the Western Pacific: An Analysis of 18 Years Ozonesonde Profiles, Earth's Future, 9, 1–9, https://doi.org/10.1029/2020EF001635, 2021.

https://doi.org/10.5194/egusphere-2026-6733
Preprint. Discussion started: 13 November 2026
© Author(s) 2026. CC BY 4.0 License.

Liang, Q., Newman, P. A., Fleming, E. L., Lait, L. R., Atlas, E., Pan, L., Kinnison, D., Western, L. M., Schauffler, S., Smith, K., Treadaway, V., Hendershot, R., Donnelly, S., and Lueb, R.: Asian Summer Monsoon Anticyclone – The Primary Entryway for Chlorinated Very-Short-Lived Substances to the Stratosphere, Geophys. Res. Lett., 52, e2024GL110248, https://doi.org/10.1029/2024GL110248, 2025.

McKenna, D. S., Grooß, J.-U., Günther, G., Konopka, P., Müller, R., Carver, G., and Sasano, Y.: A new Chemical Lagrangian Model of the Stratosphere (CLaMS): 2. Formulation of chemistry scheme and initialization, J. Geophys. Res., 107, 4256, https://doi.org/10.1029/2000JD000113, 2002a.

McKenna, D. S., Konopka, P., Grooß, J.-U., Günther, G., Müller, R., Spang, R., Offermann, D., and Orsolini, Y.: A new Chemical Lagrangian Model of the Stratosphere (CLaMS): 1. Formulation of advection and mixing, J. Geophys. Res., 107, 4309, https://doi.org/10.1029/2000JD000114, 2002b.

Meixner, K., Wagenhäuser, T., Schuck, T. J., Alber, S., Manning, A. J., Redington, A. L., Stanley, K. M., O'Doherty, S., Young, D., Pitt, J., Wenger, A., Frumau, A., Stavert, A. R., Rennick, C., Vollmer, M. K., Maione, M., Arduini, J., Lunder, C. R., Couret, C., Jordan, A., Gutiérrez, X. G., Kubistin, D., Müller-Williams, J., Lindauer, M., Vojta, M., Stohl, A., and Engel, A.: Characterization of German SF6 Emissions, ACS ES&T Air, 2, 2889–2899, https://doi.org/10.1021/acsestair.5c00234, 2025.

Membrive, O., Crevoisier, C., Sweeney, C., Danis, F., Hertzog, A., Engel, A., Bönisch, H., and Picon, L.: AirCore-HR: a high-resolution column sampling to enhance the vertical description of CH4 and CO2, Atmos. Meas. Tech., 10, 2163–-2181, https://doi.org/10.5194/amt-10-2163-2017, 2017.

Miller, B. R., Weiss, R. F., Salameh, P. K., Tanhua, T., Greally, B. R., Mühle, J., and Simmonds, P.: Medusa: a sample preconcentration and GC-MSD system for in situ measurements of atmospheric trace halocarbons, hydrocarbons and sulfur compounds, Anal. Chem., 80, 1536–1545, 2008.

Mrozek, D. J., van der Veen, C., Hofmann, M. E. G., Chen, H., Kivi, R., Heikkinen, P., and Röckmann, T.: Stratospheric Air Sub-sampler (SAS) and its application to analysis of Δ17O(CO2) from small air samples collected with an AirCore, Atmos. Meas. Tech., 9, 5607–-5620, https://doi.org/10.5194/amt-9-5607-2016, 2016.

Müller, S., Hoor, P., Bozem, H., Gute, E., Vogel, B., Zahn, A., Bönisch, H., Keber, T., Krämer, M., Rolf, C., Riese, M., Schlager, H., and Engel, A.: Impact of the Asian monsoon on the extratropical lower stratosphere: trace gas observations

https://doi.org/10.5194/egusphere-2026-6733
Preprint. Discussion started: 13 November 2026
© Author(s) 2026. CC BY 4.0 License.

during TACTS over Europe 2012, Atmos. Chem. Phys., 16, 10573–10589, https://doi.org/10.5194/acp-16-10573-2016, 2016.

Pan, L. L., Atlas, E. L., Honomichl, S. B., Smith, W. P., Kinnison, D. E., Solomon, S., Santee, M. L., Saiz-Lopez, A., Laube, J. C., Wang, B., Ueyama, R., Bresch, J. F., Hornbrook, R. S., Apel, E. C., Hills, A. J., Treadaway, V., Smith, K., Schauffler, S., Donnelly, S., Hendershot, R., Lueb, R., Campos, T., Viciani, S., D'Amato, F., Bianchini, G., Barucci, M., Podolske, J. R., Iraci, L. T., Gurganus, C., Bui, P., Dean-Day, J. M., Millán, L., Ryoo, J.-M., Barletta, B., Koo, J.-H., Kim, J., Liang, Q., Randel, W. J., Thornberry, T., and Newman, P. A.: East Asian summer monsoon delivers large abundances of very short-lived organic chlorine substances to the lower stratosphere, P. Natl. Acad. Sci. USA, 121, e2318716121, https://doi.org/10.1073/pnas.2318716121, 2024.

Ploeger, F., Günther, G., Konopka, P., Fueglistaler, S., Müller, R., Hoppe, C., Kunz, A., Spang, R., Grooß, J.-U., and Riese, M.: Horizontal water vapor transport in the lower stratosphere from subtropics to high latitudes during boreal summer, J. Geophys. Res., 118, 8111–8127, https://doi.org/10.1002/jgrd.50636, 2013.

Ploeger, F., Konopka, P., Walker, K., and Riese, M.: Quantifying pollution transport from the Asian monsoon anticyclone into the lower stratosphere, Atmos. Chem. Phys., 17, 7055–7066, https://doi.org/10.5194/acp-17-7055-2017, 2017.

Pommrich, R., Müller, R., Grooß, J.-U., Konopka, P., Ploeger, F., Vogel, B., Tao, M., Hoppe, C. M., Günther, G., Spelten, N., Hoffmann, L., Pumphrey, H.-C., Viciani, S., D'Amato, F., Volk, C. M., Hoor, P., Schlager, H., and Riese, M.: Tropical troposphere to stratosphere transport of carbon monoxide and long-lived trace species in the Chemical Lagrangian Model of the Stratosphere (CLaMS), Geosci. Model Dev., 7, 2895–2916, https://doi.org/10.5194/gmd-7-2895-2014, 2014.

Prinn, R. G., Weiss, R. F., Arduini, J., Arnold, T., DeWitt, H. L., Fraser, P. J., Ganesan, A. L., Gasore, J., Harth, C. M., Hermansen, O., Kim, J., Krummel, P. B., Li, S., Loh, Z. M., Lunder, C. R., Maione, M., Manning, A. J., Miller, B. R., Mitrevski, B., Mühle, J., O'Doherty, S., Park, S., Reimann, S., Rigby, M., Saito, T., Salameh, P. K., Schmidt, R., Simmonds, P. G., Steele, L. P., Vollmer, M. K., Wang, R. H., Yao, B., Yokouchi, Y., Young, D., and Zhou, L.: History of chemically and radiatively important atmospheric gases from the Advanced Global Atmospheric Gases Experiment (AGAGE), Earth Syst. Sci. Data, 10, 985–1018, https://doi.org/10.5194/essd-10-985-2018, 2018.

Ray, E. A., Moore, F. L., Garny, H., Hintsa, E. J., Hall, B. D., Dutton, G. S., Nance, D., Elkins, J. W., Wofsy, S. C., Pittman, J., Daube, B., Baier, B. C., Li, J., and Sweeney, C.: Age of air from in situ trace gas measurements: insights from a new technique, Atmos. Chem. Phys., 24, 12425–12445, https://doi.org/10.5194/acp-24-12425-2024, 2024.

https://doi.org/10.5194/egusphere-2026-6733
Preprint. Discussion started: 13 November 2026
© Author(s) 2026. CC BY 4.0 License.

Riese, M., Hoor, P., Rolf, C., Kunkel, D., Vogel, B., Köllner, F., Pöhlker, M., Ploeger, F., Ungermann, J., Woiwode, W., Johansson, S., Bauer, R., Barmpounis, K., Borrmann, S., Brauner, P., Clemens, J., Dragoneas, A., Ekinci, F., Emig, N., Engel, A., Eppers, O., Fadnavis, S., Friedl-Vallon, F., Geldenhuys, M., Günther, G., Grooß, J.-U., Hegglin, M. I., Hoepfner, M., Jesswein, M., Joppe, P., Kaumanns, J., Kachula, O., Keber, T., Kretschmer, E., Lachnitt, H.-C., Lauther, V., Lloyd, P. E., Molleker, S., Müller, R., Neubert, T., Ort, L., Pöschl, U., Pöhlker, C., Rapp, M., Retzlaff, M., Rhode, S., Schneider, J., Schuck, T., Sinnhuber, B.-M., Spelten, N., Strobel, J., Tomsche, L., Turhal, K., van Luijt, R., Versick, S., Voigt, C., Volk, M., von Hobe, M., Weyland, F., Zahn, A., Ziereis, H., and Zlotos, L.: Long-range transport of polluted Asian summer monsoon air to high latitudes during the PHILEAS campaign in the boreal summer 2023, B. Am. Meteorol. Soc., https://doi.org/10.1175/BAMS-D-24-0232.1, preprint, Online Publication: 8 July 2025, 2025.

Rolf, C., Vogel, B., Hoor, P., Afchine, A., Günther, G., Krämer, M., Müller, R., Müller, S., Spelten, N., and Riese, M.: Water vapor increase in the lower stratosphere of the Northern Hemisphere due to the Asian monsoon anticyclone observed during the TACTS/ESMVal campaigns, Atmos. Chem. Phys., 18, 2973–2983, https://doi.org/10.5194/acp-18-2973-2018, 2018.

Say, D., Ganesan, A. L., Lunt, M. F., Rigby, M., O'Doherty, S., Harth, C., Manning, A. J., Krummel, P. B., and Bauguitte, S.: Emissions of halocarbons from India inferred through atmospheric measurements, Atmos. Chem. Phys., 19, 9865–9885, https://doi.org/10.5194/acp-19-9865-2019, 2019.

Schuck, T. J., Lefrancois, F., Gallmann, F., Wang, D., Jesswein, M., Hoker, J., Bönisch, H., and Engel, A.: Establishing long-term measurements of halocarbons at Taunus Observatory, Atmos. Chem. Phys., 18, 16553–16569, https://doi.org/10.5194/acp-18-16553-2018, 2018.

Smit, H. G. J., Straeter, W., Johnson, B. J., Oltmans, S. J., Davies, J., Tarasick, D. W., Hoegger, B., Stubi, R., Schmidlin, F. J., Northam, T., Thompson, A. M., Witte, J. C., Boyd, I., and Posny, F.: Assessment of the performance of ECC-ozonesondes under quasi-flight conditions in the environmental simulation chamber: Insights from the Juelich Ozone Sonde Intercomparison Experiment (JOSIE), J. Geophys. Res.-Atmos., 112, D19306, https://doi.org/10.1029/2006JD007308, 2007.

Solomon, S., Mills, M., Heidt, L. E., Pollock, W. H., and Tuck, A. F.: On the evaluation of ozone depletion potentials, J. Geophys. Res.-Atmos., 97, 825–842, https://doi.org/10.1029/91JD02613, 1992.

SPARC, 2013: SPARC Report on the Lifetimes of Stratospheric Ozone-Depleting Substances, Their Replacements, and Related Species. M.K.W. Ko, P.A. Newman, S. Reimann, S.E. Strahan (Eds.), SPARC Report No. 6, WCRP-15/2013, available at www.aparc-climate.org/publications/ (last access: 29th July 2026).

https://doi.org/10.5194/egusphere-2026-6733
Preprint. Discussion started: 13 November 2026
© Author(s) 2026. CC BY 4.0 License.

Tans, P.: Fill dynamics and sample mixing in the AirCore, Atmos. Meas. Tech., 15, 1903–1916, https://doi.org/10.5194/amt-15-1903-2022, 2022.

Tarasick, D. W., Smit, H. G. J., Thompson, A. M., Morris, G. A., Witte, J. C., Davies, J., Nakano, T., Van Malderen, R., Stauffer, R. M., Johnson, B. J., Stübi, R., Oltmans, S. J., and Vömel, H.: Improving ECC Ozonesonde Data Quality: Assessment of Current Methods and Outstanding Issues, Earth Space Sci., 8, 1–27, https://doi.org/10.1029/2019ea000914, 2021.

Thompson, A. M., Smit, H. G., Witte, J. C., Stauffer, R. M., Johnson, B. J., Morris, G., Von Der Gathen, P., Van Malderen, R., Davies, J., Piters, A., Allaart, M., Posny, F., Kivi, R., Cullis, P., Anh, N. T. H., Corrales, E., Machinini, T., DaSilva, F. R., Paiman, G., Thiong'o, K., Zainal, Z., Brothers, G. B., Wolff, K. R., Nakano, T., Stübi, R., Romanens, G., Coetzee, G. J., Diaz, J. A., Mitro, S., Mohamad, M., and Ogino, S. Y.: Ozonesonde quality assurancethe josie-shadoz (2017) experience, B. Am. Meteorol. Soc., 100, 155–171, https://doi.org/10.1175/BAMS-D-17-0311.1, 2019.

Vaisala: Radiosonde RS41-D, Tech. rep., B211444EN-H, 2020.

Vömel, H., David, D. E., and Smith, K.: Accuracy of tropospheric and stratospheric water vapor measurements by the cryogenic frost point hygrometer: Instrumental details and observations, J. Geophys. Res., 112, D08305, https://doi.org/10.1029/2006JD007224, 2007.

Vömel, H., Naebert, T., Dirksen, R., and Sommer, M.: An update on the uncertainties of water vapor measurements using cryogenic frost point hygrometers, Atmos. Meas. Tech., 9, 3755–3768, https://doi.org/10.5194/amt-9-3755-2016, 2016.

Vogel, B., Günther, G., Müller, R., Grooß, J.-U., Afchine, A., Bozem, H., Hoor, P., Krämer, M., Müller, S., Riese, M., Rolf, C., Spelten, N., Stiller, G. P., Ungermann, J., and Zahn, A.: Long-range transport pathways of tropospheric source gases originating in Asia into the northern lower stratosphere during the Asian monsoon season 2012, Atmos. Chem. Phys., 16, 15301–15325, https://doi.org/10.5194/acp-16-15301-2016, 2016.

Vogel, B., Müller, R., Günther, G., Spang, R., Hanumanthu, S., Li, D., Riese, M., and Stiller, G. P.: Lagrangian simulations of the transport of young air masses to the top of the Asian monsoon anticyclone and into the tropical pipe, Atmos. Chem. Phys., 19, 6007–6034, https://doi.org/10.5194/acp-19-6007-2019, 2019.

https://doi.org/10.5194/egusphere-2026-6733
Preprint. Discussion started: 13 November 2026
© Author(s) 2026. CC BY 4.0 License.



Vogel, B., Lauther, V., Köllner, F., Ekinci, F., Rolf, C., Strobel, J., van Luijt, R., Volk, C. M., Borrmann, S., Dragoneas, A., Eppers, O., Molleker, S., Hoor, P., Ort, L., Weyland, F., Zahn, A., Clemens, J., Günther, G., Kachula, O., Müller, R., Ploeger, F., and Riese, M.: Continental and marine source regions contributing to the outflow of the Asian summer monsoon anticyclone during the PHILEAS campaign in summer 2023, Atmos. Chem. Phys., 26, 6283–6319, https://doi.org/10.5194/acp-26-6283-2026, 2026.

Vojta, M., Plach, A., Annadate, S., Park, S., Lee, G., Purohit, P., Lindl, F., Lan, X., Mühle, J., Thompson, R. L., and Stohl, A.: A global re-analysis of regionally resolved emissions and atmospheric mole fractions of SF6 for the period 2005–2021, Atmos. Chem. Phys., 24, 12465–12493, https://doi.org/10.5194/acp-24-12465-2024, 2024.

Volk, C. M., Elkins, J. W., Fahey, D. W., Salawitch, R. J., Dutton, G. S., Gilligan, J. M., Proffitt, M. H., Loewenstein, M., Podolske, J. R., Minschwaner, K., Margitan, J. J., and Chan, K. R.: Quantifying transport between the tropical and mid-latitude lower stratosphere, Science, 272, 1763–1768, 1996.

Wagenhäuser, T., Engel, A., and Sitals, R.: Testing the altitude attribution and vertical resolution of AirCore measurements with a new spiking method, Atmos. Meas. Tech., 14, 3923–-3934, https://doi.org/10.5194/amt-14-3923-2021, 2021.

Wagenhäuser, T., Jesswein, M., Keber, T., Schuck, T., and Engel, A.: Mean age from observations in the lowermost stratosphere: an improved method and interhemispheric differences, Atmos. Chem. Phys., 23, 3887–3903, https://doi.org/10.5194/acp-23-3887-2023, 2023.

Western, L. M., Rigby, M., Mühle, J., Krummel, P. B., Lunder, C. R., O'Doherty, S., Reimann, S., Vollmer, M. K., Young, D., Adam, B., Fraser, P. J., Ganesan, A. L., Harth, C. M., Hermansen, O., Kim, J., Langenfelds, R. L., Loh, Z. M., Mitrevski, B., Pitt, J. R., Salameh, P. K., Schmidt, R., Stanley, K., Stavert, A. R., Wang, H.-J., Weiss, R. F., and Prinn, R. G.: Global emissions and abundances of chemically and radiatively important trace gases from the AGAGE network, Earth Syst. Sci. Data, 17, 6557–6582, https://doi.org/10.5194/essd-17-6557-2025, 2025.

Wetzel, G., Friedl-Vallon, F., Glatthor, N., Grooß, J.-U., Gulde, T., Höpfner, M., Johansson, S., Khosrawi, F., Kirner, O., Kleinert, A., Kretschmer, E., Maucher, G., Nordmeyer, H., Oelhaf, H., Orphal, J., Piesch, C., Sinnhuber, B.-M., Ungermann, J., and Vogel, B.: Pollution trace gases C2H6, C2H2, HCOOH, and PAN in the North Atlantic UTLS: observations and simulations, Atmos. Chem. Phys., 21, 8213–8232, https://doi.org/10.5194/acp-21-8213-2021, 2021.

Yan, X., Konopka, P., Ploeger, F., and Podglajen, A.: Transport into the polar stratosphere from the Asian monsoon region, Atmos. Chem. Phys., 25, 1289–1305, https://doi.org/10.5194/acp-25-1289-2025, 2025.

https://doi.org/10.5194/egusphere-2026-6733
Preprint. Discussion started: 13 November 2026
© Author(s) 2026. CC BY 4.0 License.



Zhang, X., An, M., Chen, Z., Jiang, P., Bai, F., Zhao, X., Xu, W., and Hu, J.: Chlorinated VSLSs Surpass HCFCs in CFC-11-Equivalent Emissions for Ozone Layer Depletion in China, Nat. Commun., https://doi.org/10.1038/s41467-026-75080-y, 2026.